공학석사학위논문

SI 엔진에서 열 경계 조건이 효율에 미치는 영향에 대한 연구

A Study on Effect of Thermal Boundary Conditions on Efficiency in Spark-ignited Engine

2020년 2월

서울대학교 대학원

기계항공공학부

신 석 원

SI 엔진에서 열 경계 조건이 효율에 미치는 영향에 대한 연구

A Study on Effect of Thermal Boundary Conditions on Efficiency in Spark-ignited Engine

지도교수 민 경 덕

이 논문을 공학석사 학위논문으로 제출함

2019년 10월

서울대학교 대학원

기계항공공학부

신 석 원

신석원의 공학석사 학위논문을 인준함

2019년 12월

위 원 장 _____(인)

부위원장 _____(인)

위 원 _____(인)

Abstract

A Study on Effect of Thermal Boundary Conditions on Efficiency in Spark-ignited Engine

Sukwon Shin

Department of Mechanical and Aerospace Engineering

The Graduate School

Seoul National University

Globally, enacted regulations on vehicle are getting stricter, enforcing efficiency improvement of engines. Even though knocking phenomenon has been a strong obstacle in development of higher efficiency engine, it can be suppressed if the temperature of the working fluid can be lowered by changing the thermal boundary conditions of an engine.

In this study, insulated intake port and piston cooling oil-jet were selected as methods for modifying thermal boundary conditions. Insulation in intake port can nearly block heat transfer to incoming air through use of material with extremely low thermal conductivity. Piston cooling oil-jet lowers in-cylinder temperature by intensifying cooling loss from combustion chamber to lubricating oil at piston. Experiments were conducted to investigate the feasibility of these

methods as efficiency improvement strategies.

By implementation of insulated intake port, air temperature reduction effect was verified. Accordingly, MBT region was expanded and efficiency increased at fixed fuel rate condition. Moreover, CFD simulation was conducted to examine possible additional improvement by complete insulation.

Piston cooling oil-jet tests were executed at two different speeds with fixed fuel rates. The outcome indicated that the use of various oil-jets types commonly had positive influences on efficiency, even though the magnitude and trend differed at two different operating conditions.

In overall, this study has confirmed that the modification of thermal boundary conditions in intake port and piston can accommodate efficiency improvement. As a result, it is expected that this study can serve as a guidance to development of higher efficiency engine.

Keyword : Efficiency improvement, Thermal boundary condition, Intake port insulation, Piston cooling oil-jet, Cooling Gallery, Undercrown, SI engine

Student Number : 2018-27312

Table of Contents

List of Tables

List of Figures

Nomenclature

Acronyms

ATDC	after top dead center
BDC	bottom dead center
BTDC	before top dead center
CA	crank angle
CFD	computational fluid dynamics
CG	cooling gallery
CR	compression ratio
CVVT	continuously variable valve timing
EVC	exhaust valve closing
EVO	exhaust valve opening
GMEP	gross mean effective pressure
IMEP	indicated mean effective pressure
IVC	intake valve closing
IVO	intake valve opening
KLSA	knock limit spark advance
LPG	liquid petroleum gas
MAPO	maximum amplitude of pressure oscillation
MBT	maximum brake torque
MEP	mean effective pressure
MFB50	mass fraction burned 50 %

PFI	port fuel injection
PMEP	pumping mean effective pressure
S/B	stroke/bore
SI	spark ignition
TDC	top dead center
TVE	threshold value exceed
UC	undercrown
UC+CG	simultaneous injection
WOT	wide open throttle

Chapter 1. Introduction

1.1 Background

1.1.1 Need for Engine Efficiency Improvement

Carbon dioxide, which is a greenhouse gas that accelerates global warming, is being produced at increasing rate annually (Figure 1.1.1 a) [1]. As a result, especially for past few decades, the average global temperature has risen dramatically (Figure 1.1.1 b). When defining the ratio of anthropogenic carbon dioxide emission by origins, transport sector is responsible for 23 % of the total production (Figure 1.1.2) [2]. Of this great portion, on-road vehicle takes up 73.9 %, which equals to approximately 17 % of entire carbon dioxide quantity. As a measure to impede the deterioration of contamination, major countries have legislated regulations on emissions and fuel economy of vehicles. To meet the emission requirements in near future, it is inevitable to lower carbon dioxide emissions by 16 % to as high as 49 % compared to 2010 in major countries (Figure 1.1.3) [2]. Regarding fuel economy, 24.3km/L has to be achieved by 2020 in South Korea (Figure 1.1.4) [3]. This corresponds to 51 % improvement from 2015, in which requirement was 16.1 km/L.

To satisfy the regulations, improvement of engine thermal

efficiency is inevitable and there has been tremendous effort to overcome the challenge. For instance, increasing compression ratio of the engine is a simple, straight-forward method for efficiency enhancement. However, knocking phenomenon stands as a major obstacle. Knock occurs as a result of an auto-ignition, in form of detonation, of air-fuel mixture before the normal flame approaches due to high temperature and pressure of the surrounding. When knock occurs, it could result in critical and permanent damage to engine. Therefore, knock is being suppressed despite its hindrance to efficiency improvement.

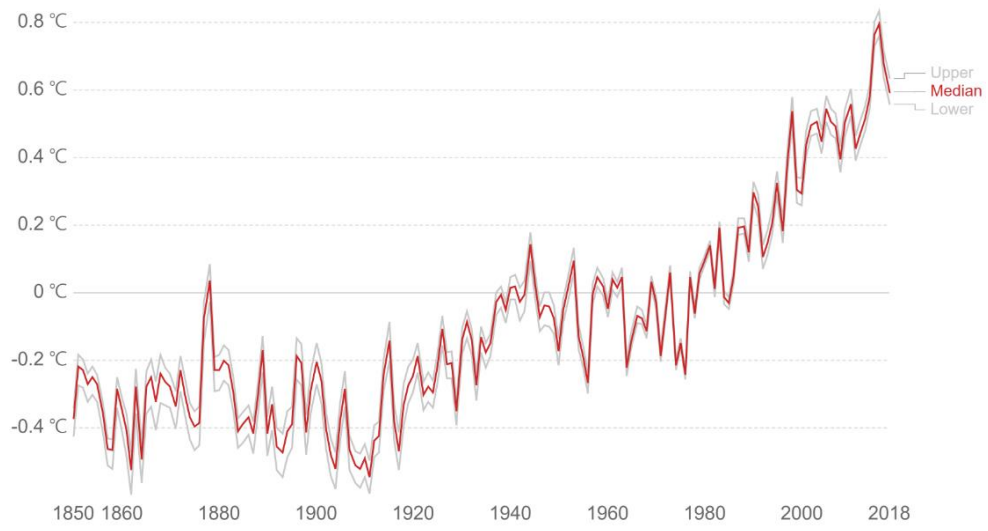

(a)

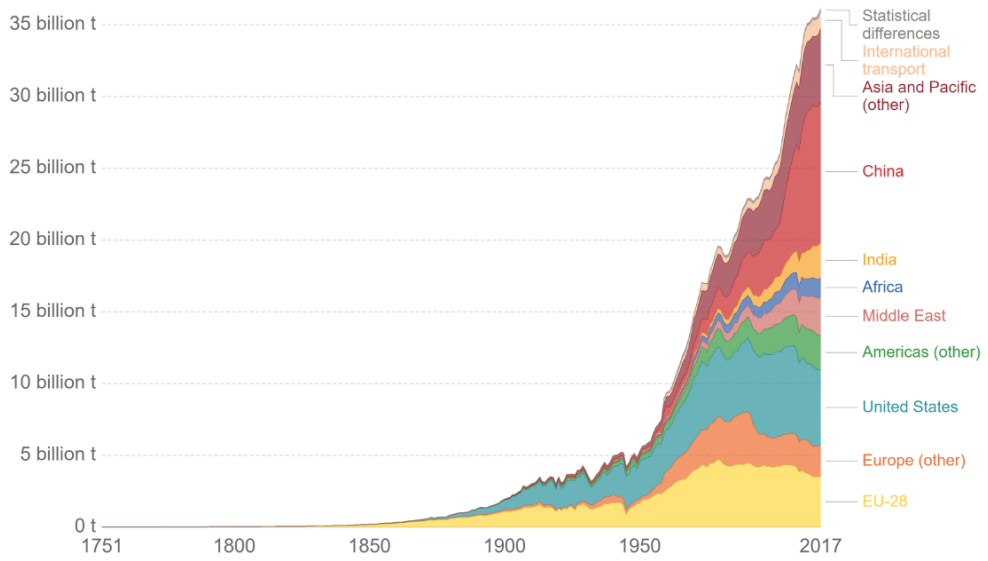

(b)

Figure 1.1.1 Annual global average temperature rise (a) and total carbon dioxide emission (b) [1]

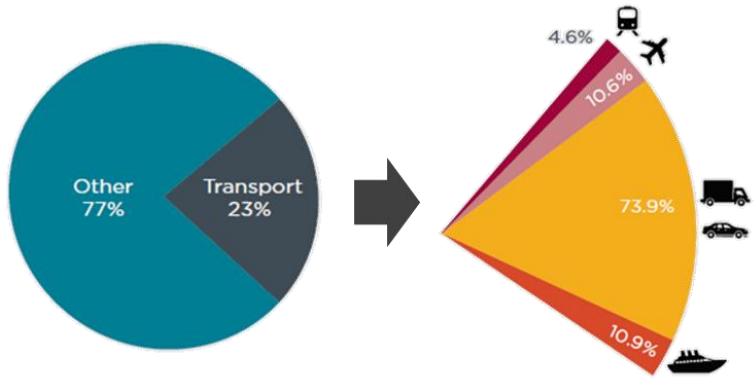

Figure 1.1.2 Ratio of anthropogenic carbon dioxide emissions by origins [2]

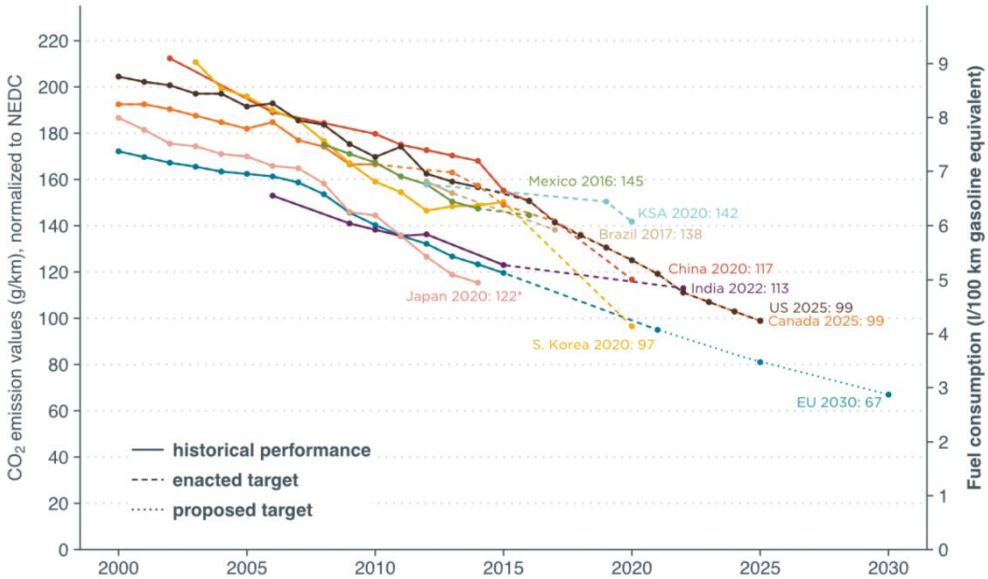

Figure 1.1.3 Global carbon dioxide emission standards [2]

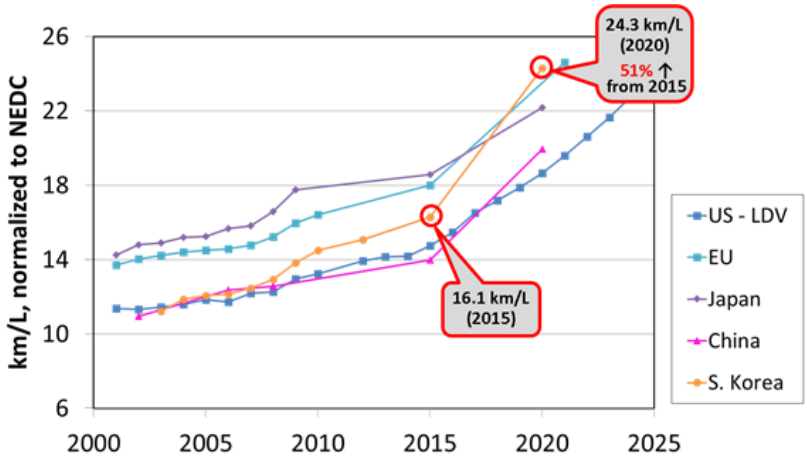

Figure 1.1.4 Global fuel economy standards

1.1.2 Heat Transfer Reduction Methods

Since knocking occurs due to high temperature and pressure during combustion, it can be reduced by lowering the initial temperature of the fresh charge. Assuming constant ambient temperature, heat transfer from engine surfaces to the fresh mixture would have to be decreased. Out of major engine parts, intake port accounts for approximately 40 % of the total heat transfer to incoming air (Figure 1.1.5) [4]. When only considering cylinder inner walls excluding intake port, piston and liner occupy two largest portions of total heat transfer to working fluid during IVO to IVC (Figure 1.1.6) [5]. Depending on operating conditions, piston can be held responsible for up to 24.12 %. Since intake port and piston are the two major sources of heating of incoming air, knocking could be significantly reduced if thermal boundary conditions at these two parts can be changed.

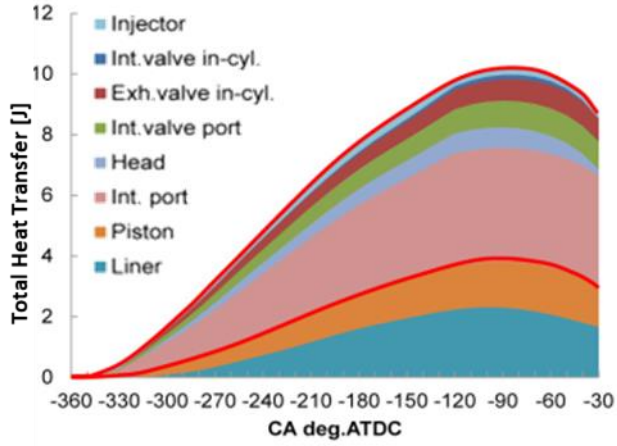

Figure 1.1.5 Heat transfer from major engine parts [4]

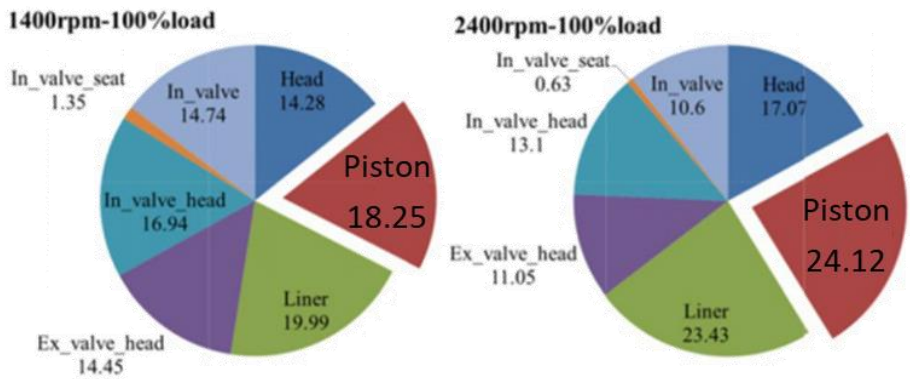

Figure 1.1.6 Heat transfer from cylinder inner walls [5]

In case of intake port, alteration of boundary conditions can be accomplished by insulation, which blocks heat transfer due to extremely low thermal conductivity. Insulation can be done by either coating or replacement of part with insulating material. Even though coating is advantageous in that insulation can be done on entire parts, only thin layer of coating can be formed. This drawback leads to durability issue as coating gets peeled off gradually. In contrast, replacing thicker part of the intake port made with insulating material can serve its function permanently.

For piston, implementation of oil-jet is a feasible option. There exist two major types of oil-jets, undercrown and cooling gallery oil-jets. Undercrown oil-jet simply injects oil to undercrown of the piston and oil falls directly back. In comparison, cooling gallery oil-jet injects oil to cooling gallery inlet so that oil can travel through the gallery and fall down at the exit, as shown in Figure 1.1.7. Regardless of the type, when oil is injected to bottom side of the piston from the oil-jet, heat of the combustion chamber is additionally shifted away to the oil, decreasing the in-cylinder temperature.

From these methods, knocking tendency of fresh charge would be mitigated, enabling combustion at preferable condition. As a result, efficiency improvement can be expected.

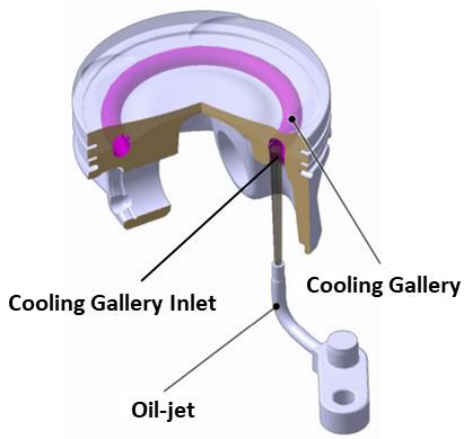

Figure 1.1.7 Concept of cooling gallery oil-jet [6]

1.2 Previous Researches

There have been numerous studies concerning both intake port insulation and piston cooling oil-jet. The positive influence of reduced intake temperature, simply by changing ambient temperature is widely known [7, 8]. However, the effect of intake port insulation is controversial. Several studies reported increase in efficiency and performance by reduced intake air temperature from intake port insulation [4, 9-11]. In contrast, Hakansson observed temperature reduction by insulated port as well, but claimed deterioration of fuel consumption due to fuel conversion efficiency issue [12].

Regarding oil-jet, plenty of previous researches proved temperature reduction impact in diesel engine. Cooling effect of oil-jet has been seen by temperature change [13, 14]. As a result, fuel consumption saving with cooling gallery oil-jet was verified [15]. Unlike abundancy of oil-jet researches in diesel engine, research in gasoline engine is relatively rare. Only recently in 2017, Maeyama et al. reported 0.5 % efficiency increase using cooling gallery in gasoline engine [6]. Another scarcity in oil-jet researches is comparison between oil-jet types as existing studies are heavily focused on cooling gallery oil-jet. Few studies claim that cooling gallery oil-jet is more effective in cooling compared to undercrown oil-jet due to larger cooling area, absorption of heat in upper part of piston that is

hotter, and more effective heat transfer by cocktail-shaker effect [14, 16-18]. However, none of them have proven experimentally yet.

1.3 Research Objectives

In spite of tremendous efforts to improve engine efficiency by intake port insulation and piston cooling oil-jets, there still exist gray-areas and room for further extension of knowledge. Therefore, this paper has aimed to fill up the missing parts in this field of study. The objectives are as follow:

1) Effect of insulated intake port was experimentally tested to clarify the controversial effect on efficiency in existing studies.

2) Various oil-jet type combinations were compared experimentally to extend the missing knowledge regarding effect of oil-jet types on efficiency in spark-ignited engine.

Chapter 2. Methodology

2.1 Experimental Configuration

2.1.1 Test Cell Apparatus

The experiments were operated with 190kW ELIN AC dynamometer (Figure 2.1.1). Engine oil and coolant were each controlled by individual controllers. Fuel flow rate was measured by OVAL Coriolis type CA001 fuel flowmeter. Then, measured flow rate was graphed and injection duration was adjusted accordingly in LabView. Ignition timing was also controlled through LabView, coupled with 3600 ticks rotary encoder. INCA program was used to manipulate valve timing of CVVT and throttle.

Pressure was measured at intake and in-cylinder. Intake manifold pressure was measured by Kistler 4045A2 absolute pressure sensor and in-cylinder pressure was measured by Kistler 6056A piezoelectric pressure sensor. Cylinder pressure was analyzed by Indicom at real-time for combustion characteristics monitoring and the logged Indicom data was used for further analysis. Exhaust emissions were measured by Horiba MEXA 7100DEGR and air-fuel equivalence ratio was maintained at 1 by lambda monitoring with Horiba MEXA-110 λ.

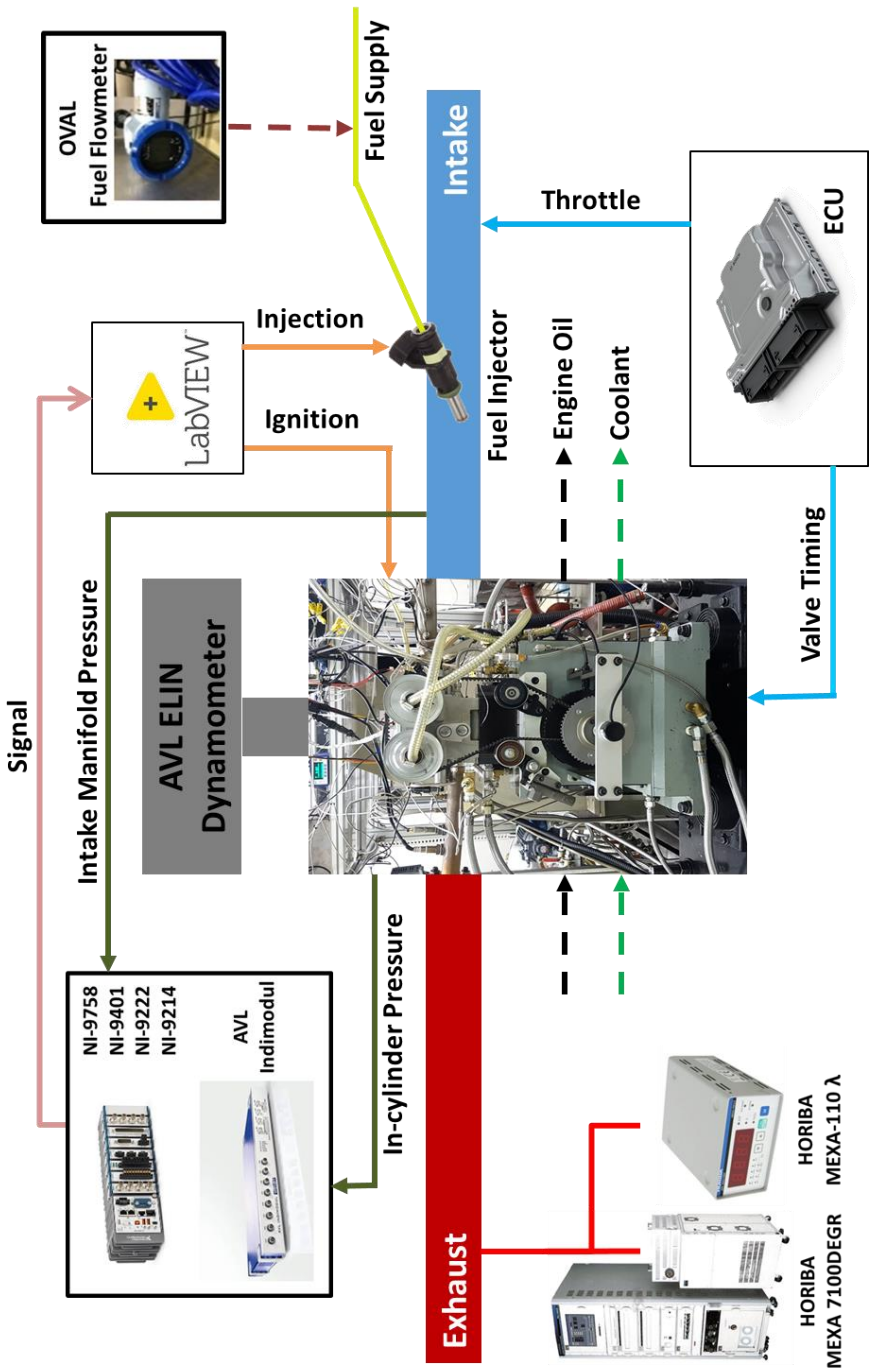

Figure 2.1.1 Test cell configuration

2.1.2 Single-cylinder Research Engine

Single cylinder naturally aspirated engine was used for the test (Table 2.1.1). Valve timing was variable with dual CVVT system. Total displacement is 499.8 cc with stroke 97 mm, bore 81 mm, and S/B ratio of 1.2. Geometric compression ratios are 11.2 and 12, depending on piston top shape. Injection system differed depending on the fuel type. Gasoline was injected by two gasoline injectors at intake port and LPG was injected by single LPG injector at manifold after throttle. Gasoline was pressurized to 5 bar using fuel pump, while LPG was pressurized to 5 bar using high pressure N2 gas (Figure 2.1.2).

Table 2.1.1 Test engine specification

Type of engine	Single-cylinder N/A Dual CVVT
Displacement [cc]	499.8
Stroke [mm]	97
Bore [mm]	81
Stroke-to-Bore ratio	1.2
Compression ratio	11.2 / 12
Injection system	LPG: Single-point Gasoline: Dual PFI
Number of Valves	4
Maximum Valve Lift	10 mm

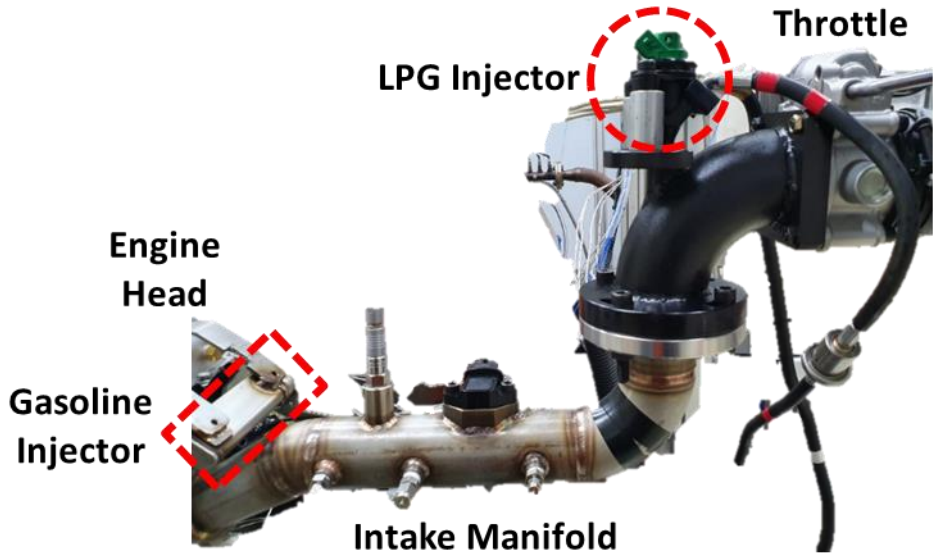

Figure 2.1.2 Fuel injection system

2.1.3 CFD Modelling

CFD was conducted by Star CD version 4.28 (Table 2.1.2). Total of 1162713 grids were used with grid size of 1 mm^3. k−ε RNG model was used for turbulence and Angelberger wall function was implemented for wall heat transfer. Boundary conditions were unified to 300 K.

Table 2.1.2 CFD specification

Program	Star CD 4.28
Grid #	1,162,713
Grid Size	$1mm^3$
Turbulence Model	k-ε RNG model
Wall Heat Transfer	Angelberger wall function

2.2 System for Alteration of Thermal Boundary Conditions

2.2.1 Intake Port Insulation

As mentioned in section 1.1.3, insertion of replacement part is advantageous compared to coating. Therefore, replacement method is widely used for researches and, thus, was selected as an insulation option for this study. Figure 2.2.1 illustrates the insulating material, in black color, was inserted into the intake port of the test engine, in comparison to standard intake port. For intake port temperature measurement, two thermocouples were installed at port mid and out as shown in Figure 2.2.2.

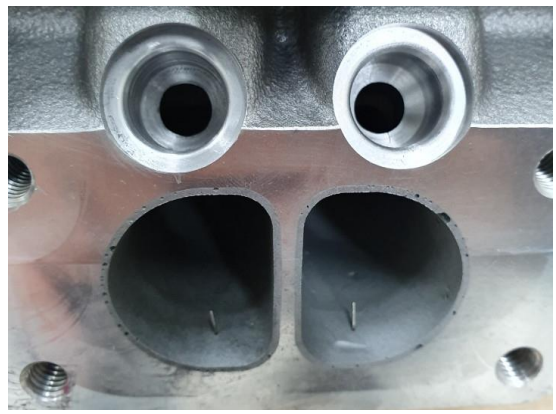

(a)

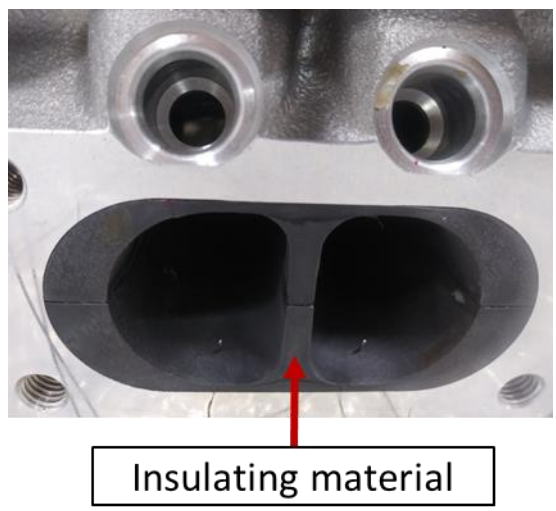

(b)

Figure 2.2.1 Standard intake port (a) and intake port replaced with insulating material (b)

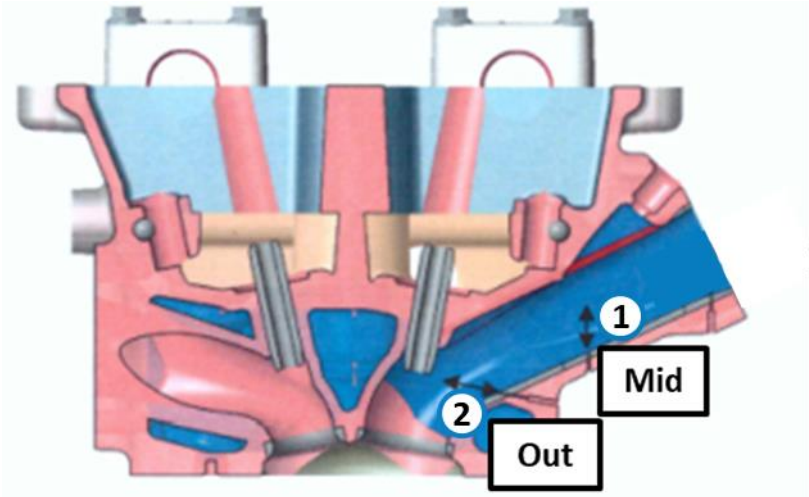

Figure 2.2.2 Intake port temperature measurement location

2.2.2 Piston Cooling Oil-jet

Both undercrown oil-jet and cooling gallery oil-jet were fixed to the engine body block on the intake side. Undercrown oil-jet targets the bottom side of the piston, illustrated in red circle in Figure 2.2.3. Cooling gallery oil-jet tip, where oil is injected, was designed to align with the cooling gallery inlet of the piston.

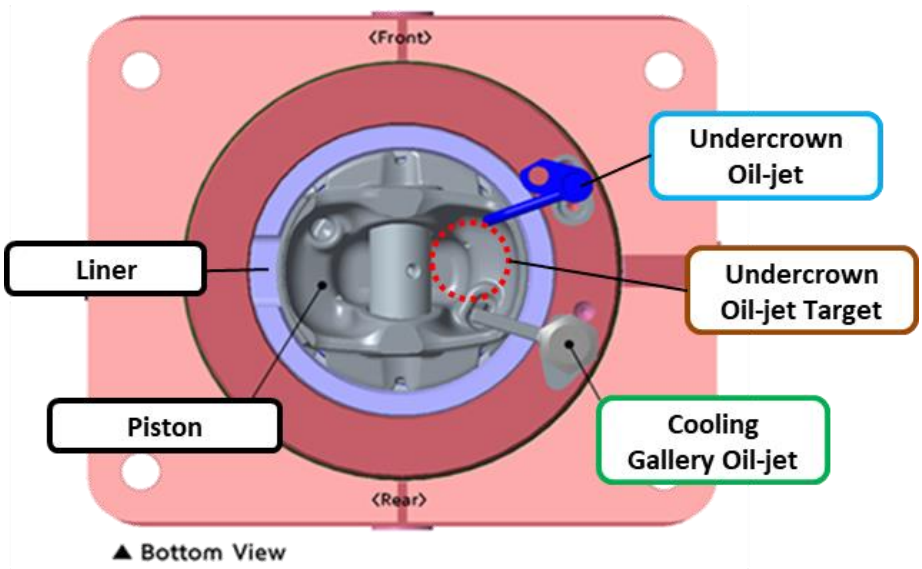

Figure 2.2.3 Oil-jets installation location

2.3 Test Condition

2.3.1 Common Condition

Oil and coolant water temperature was maintained at 85 ℃. Knocking was distinguished based on MAPO and TVE method with threshold value of 0.5 bar. It was considered KLSA when frequency of classified knock occurrence was 10 % of total cycle. Spark timing was always fixed to KLSA for maximum efficiency, while protecting engine from severe engine damage at the same time.

2.3.2 Experiment Condition of Insulated Intake Port

Two kinds of experiment were conducted regarding intake port insulation. First is the expansion of MBT region. It is widely known that MBT occurs when MFB50 is around 8 ATDC CA. However, above certain load, spark timing is retarded excessively to protect from knock and, thus, MFB50 locates beyond 8 ATDC CA (Figure 2.3.1). This deteriorates thermal efficiency. Therefore, MBT region borderline was defined as a load point in which KLSA and MBT timing is simultaneously achieved. By comparing the borderlines of MBT region, it is possible to indirectly examine which hardware is advantageous at maintaining high efficiency in wider operating range. To figure out this boundary point, the experiment was conducted at

each standard and insulated intake port. Piston with geometric compression ratio of 11.2 was used (Table 2.3.1).

Second part was an efficiency comparison experiment. For ease of comparison, the test was proceeded at fixed fuel rate, as elevation of output is equal to efficiency improvement with equivalent input fuel amount. The fuel rate was 25.8 mg/cycle. Piston with compression ratio of 12 was used.

All tests were run at 1500 rpm. Because LPG evaporates rapidly, all intake port experiment was carried out using LPG as a fuel to purely test the effect of intake port insulation, avoiding fuel conversion efficiency issue quoted by Hakansson [12]. Valve timings were adjusted to values in Table 2.3.2 by CVVT.

Ambient temperature difference between standard port and insulated port cases was always kept within 1 ℃. When analyzing temperature reduction effect of intake port insulation relative to standard intake port, the reduction gap was corrected by considering the ambient temperature difference between the tests.

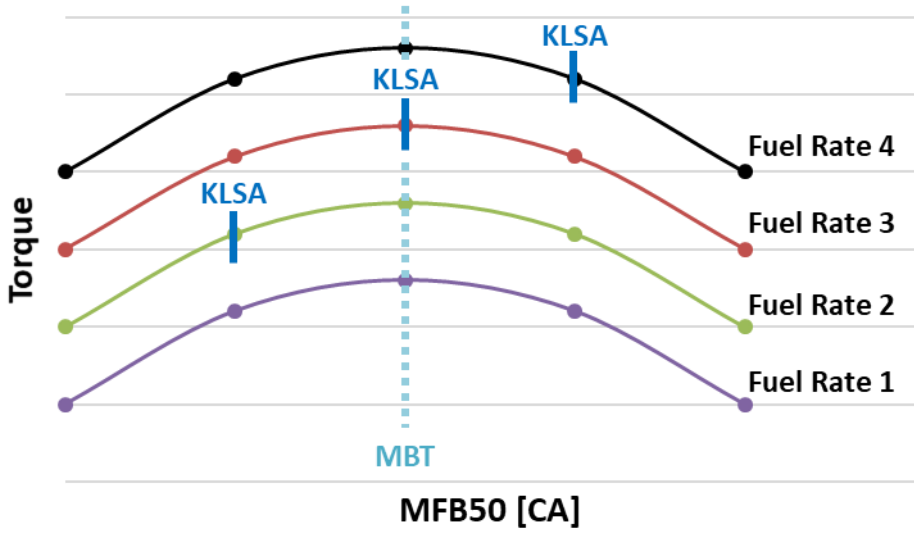

Figure 2.3.1 KLSA at different fuel rates

Table 2.3.1. Experiment condition of insulated intake port

Method	Fuel	Piston	Engine Operating Point		Comparison	
		CR*	Engine Speed [RPM]	Fixed Condition	Base	Variations
Intake Port Insulation	LPG	11.2	1500	MFB50 @ aTDC 8 CA	Standard intake port	Insulated intake port
		12		25.8 mg/cyc (~ IMEP 9.0 bar)		

Table 2.3.2 Valve timings for insulated intake port experiment

Valve Open/Close	Timing [ATDC CA]
EVO	−247
EVC	−1
IVO	−13
IVC	230

2.3.3 Experiment Condition of Oil-jet

Oil-jet experiments were executed at two engine speeds with fixed fuel rate condition (Table 2.3.3). At 1500 rpm, fuel rate was given as 32.3 mg/cycle and, at 2500 rpm, 27.5 mg/cycle was supplied. The fuel rates were selected as such to test the influence of engine speed at similar loads of approximately 8.8 bar. At both engine speeds, results were compared between no oil-jet (base condition), undercrown (UC) oil-jet, cooling gallery (CG) oil-jet, and simultaneous (UC+CG) injection. Oil-jet pressure was varied as 1, 2, 3, 3.8(3.6) bar to check the dependency of piston temperature cooling on oil flow rate [13]. In single oil-jet test, maximum oil pressure was 3.8 bar. However, at simultaneous injection, maximum possible oil pressure was 3.6 bar at each oil-jet due oil pump performance limit from massive total oil flow.

CR 11.2 piston was used in both experiments to keep the conditions as same as possible for comparison between two engine speeds. Gasoline was used for oil-jet experiment due to ease of supply and replenishment. Valve timings are shown in Table 2.3.4.

Table 2.3.3. Experiment condition of oil-jet

Method	Fuel	Piston	Engine Operating Point		Comparison			
		CR*	Engine Speed [RPM]	Fixed Condition	Base	Variations		
Oil-jet	Gasoline	11.2	1500	32.3 mg/cyc (~ IMEP 8.8 bar)	No oil-jet injection	Undercrown (UC) oil-jet	Cooling gallery (CG) oil-jet	Simultaneous (UC+CG)
			2500	27.5 mg/cyc (~ IMEP 8.8 bar)				

Table 2.3.4 Valve timings for oil-jet experiment

Valve Open/Close	Timing [ATDC CA]
EVO	-241
EVC	3
IVO	-52
IVC	189

Chapter 3. Results of Insulated Intake Port

3.1 Air Temperature Reduction

First, the temperature difference by insulation was measured at 1500 rpm WOT motoring. The temperature reduction magnitude was corrected considering ambient temperature difference. It was unexpected that air temperature starts to decline at manifold since identical manifold was used for insulated port experiment compared to standard port experiment (Figure 3.1.1). It is inferred that this phenomenon occurred because with insulated port, heat transfer is blocked not only from port to incoming air, but also from port to manifold by conduction. Therefore, due to smaller temperature gradient, less heat transfer occurred from manifold to incoming air. At intake port, significant reduction of intake air temperature was observed. Especially at port out, which is the main interest point since its location is right before the entrance to the cylinder, 3.4 ℃ reduced air temperature was measured by insulation. From this, the temperature reduction effect of insulated intake port was confirmed

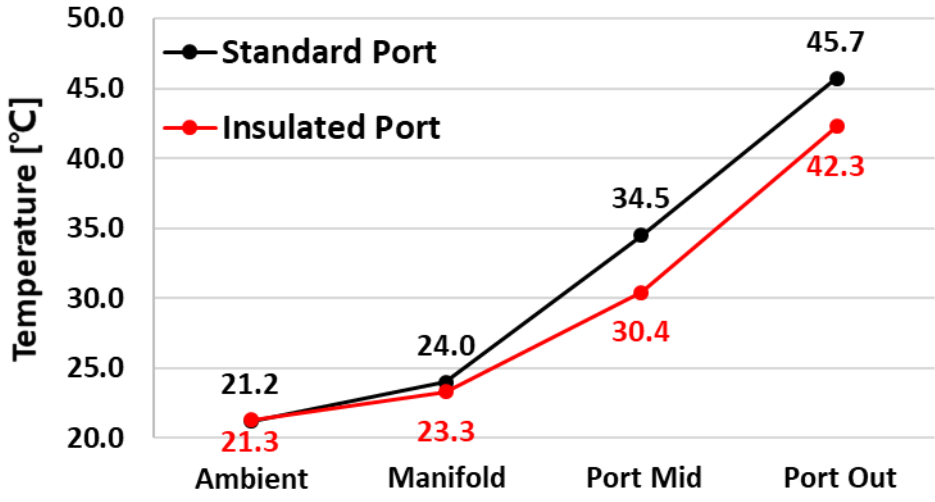

(a)

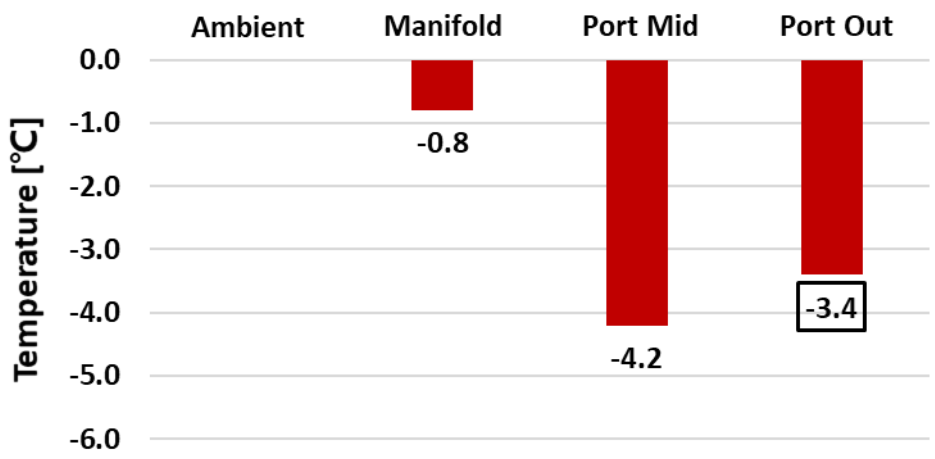

(b)

Figure 3.1.1 Measured air temperature (a) and corrected air temperature reduction (b) for motoring

3.2 Expansion of MBT Region

In combustion experiment, LPG is injected before the location of manifold air temperature measurement, so temperature decreases at manifold. Regardless, intake air temperature could be lowered by 3.6 ℃ at port out (Figure 3.2.1), similar to motoring condition. As a result, knocking was reduced since overall in-cylinder temperature during the combustion would also have declined with lower starting point. Accordingly, to qualify for KLSA condition, increment of load was essential to increase in-cylinder temperature and pressure so that more knocking cycles could be generated (Figure 3.2.2). At higher load, burn duration shortens due to enhanced flame propagation speed at higher temperature, leading to advanced MFB50 at the same ignition timing. To satisfy MFB50 requirement at 8 ATDC CA, ignition timing has to be retarded. Knocking was additionally reduced as a consequence, so load was raised once more.

Ultimately, the load point satisfying KLSA and MBT timing simultaneously was found with 2.9 CA shortened burn duration and 0.7 CA retarded ignition timing in the insulated intake port. Fuel could be injected more by 2.84 % in total. This point is 1.79 % higher in IMEP compared to the borderline in the standard intake port. While operating at the region between these two points, engine with insulated port can maintain MBT, whereas engine with standard port

would have to operate at relatively lower efficiency spark timing for protection of the engine from knock. Therefore, over this range of operating points, it is expected that the engine with intake port insulation would perform with enhanced efficiency.

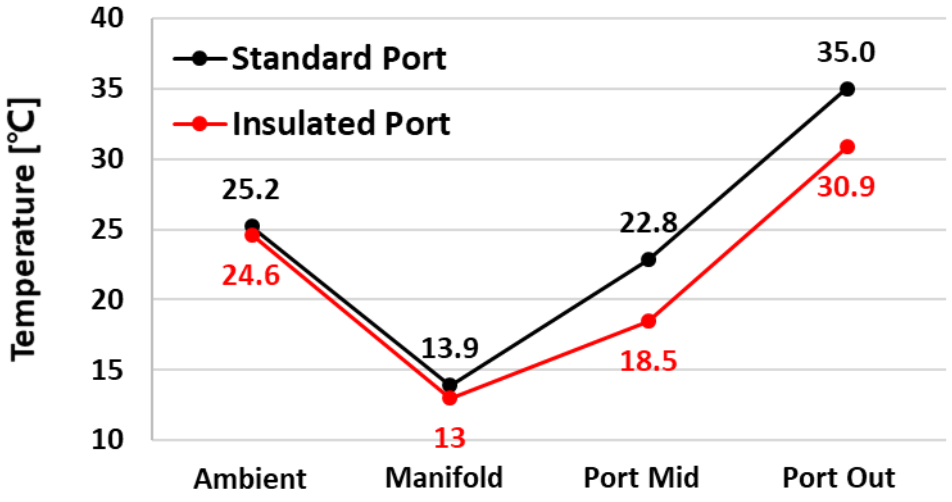

(a)

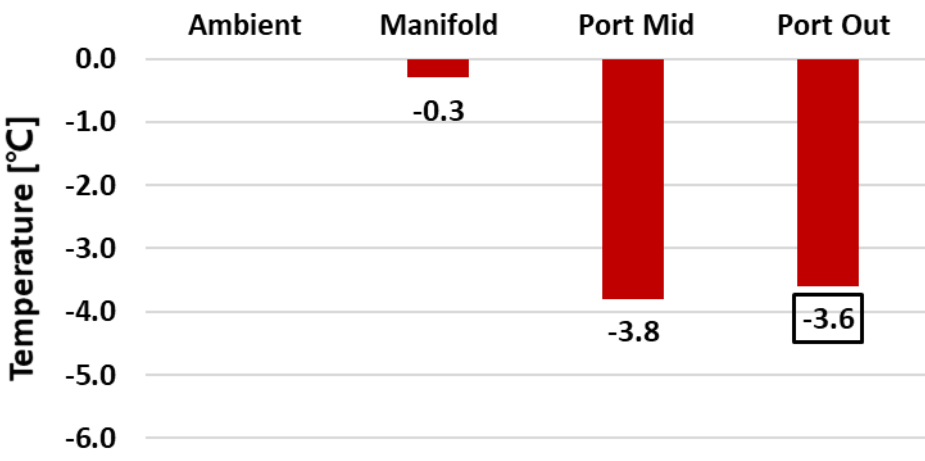

(b)

Figure 3.2.1 Measured air temperature (a) and corrected air temperature reduction (b) for MBT region expansion

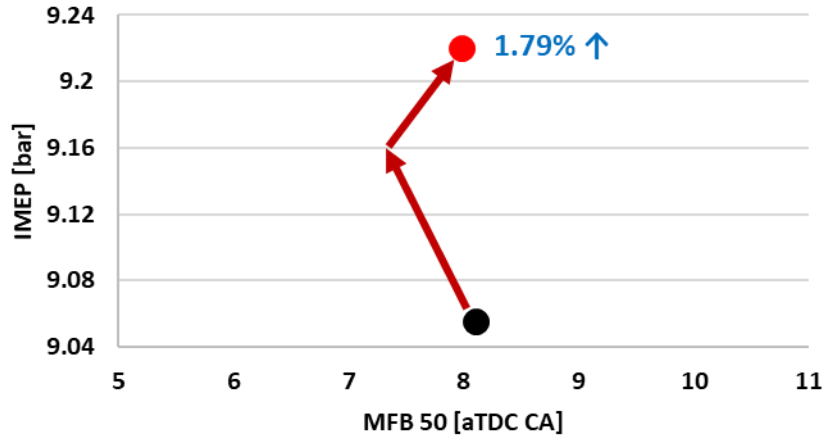

Figure 3.2.2 Extended MBT region boundary point

3.3 Efficiency Improvement

For fixed fuel rate experiment, 2.1 ℃ drop at port out was observed for the intake air temperature by insulation (Figure 3.3.1). Followed by reduced knocking, spark timing could be further advanced by 1.6 CA to reach new KLSA. As a result, overall combustion characteristics changed. For example, peak pressure was increased by 3.5 bar and located at advanced crank angle. Furthermore, despite 0.4 CA elongated burn duration due to cooler starting temperature, MFB50 was advanced from 14.1 to 11.8 ATDC CA, which is closer to MBT (8 ATDC CA). By combustion closer to MBT timing, more efficient combustion occurred, which led to MEP gain in expansion stroke (Figure 3.3.2). Ultimately, IMEP was increased by 0.29 % (Figure 3.3.3). Given equivalent fuel rate, insulated port produced more output, so it can be concluded that application of intake port could improve efficiency.

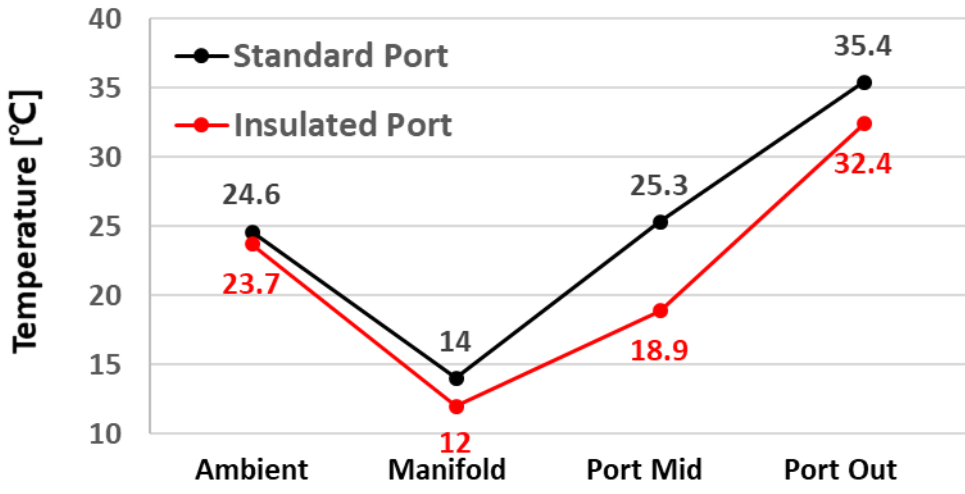

(a)

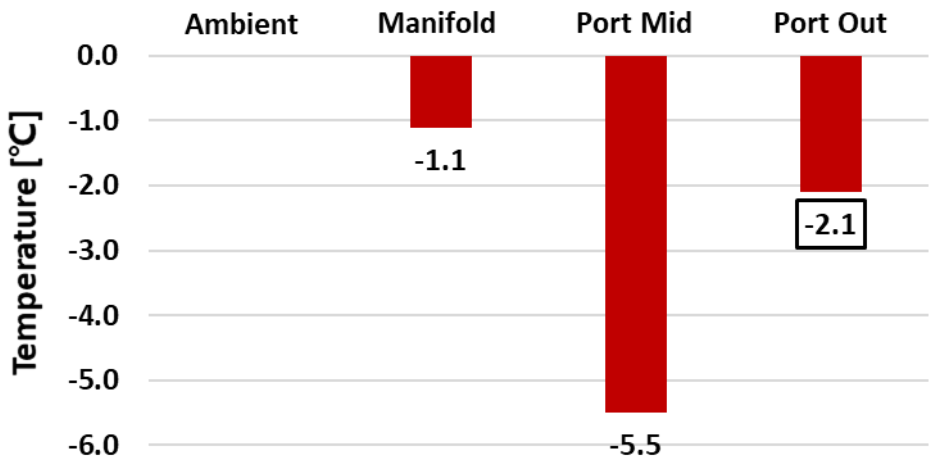

(b)

Figure 3.3.1 Measured air temperature (a) and corrected air temperature reduction (b) for efficiency improvement

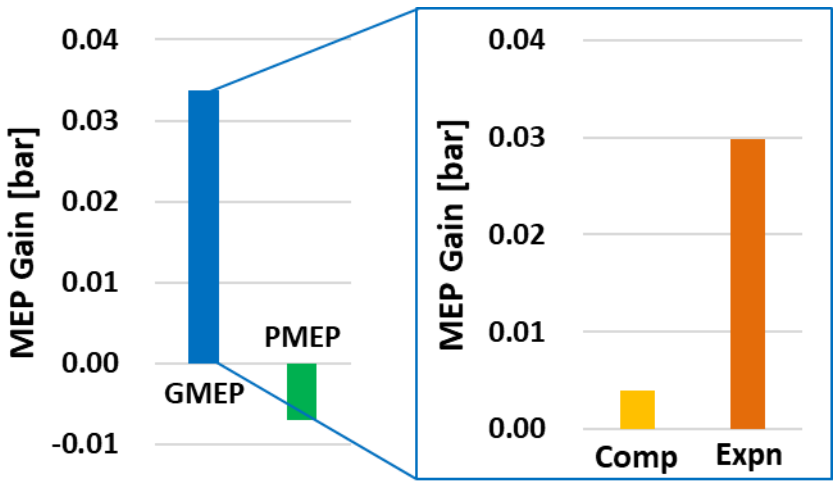

Figure 3.3.2 Sources of MEP Gain by Insulated Intake Port

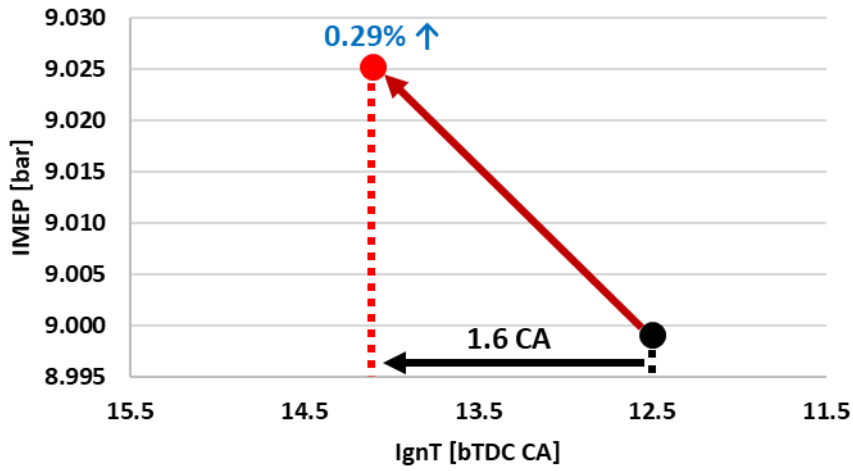

Figure 3.3.3 Ignition timing advance and IMEP gain by insulated intake port

3.4 Imperfect Insulation Issue

Insulating material was missing on the upper side of intake port after injector holes, corresponding to inside of the circle in Figure 3.4.2. This imperfect insulation was inevitable due to manufacturing hardship caused by complex curvature design in intake port. As the top of the intake port was exposed to air, like standard port, it was expected that heat transfer to incoming air would not be perfectly blocked.

As a result, from motoring case to combustion experiments, it was commonly observed that the temperature reduction gap by intake port insulation decreased as air moved from port mid to port out (Figure 3.4.1). This fact suggests that heat transfer did occur along the path.

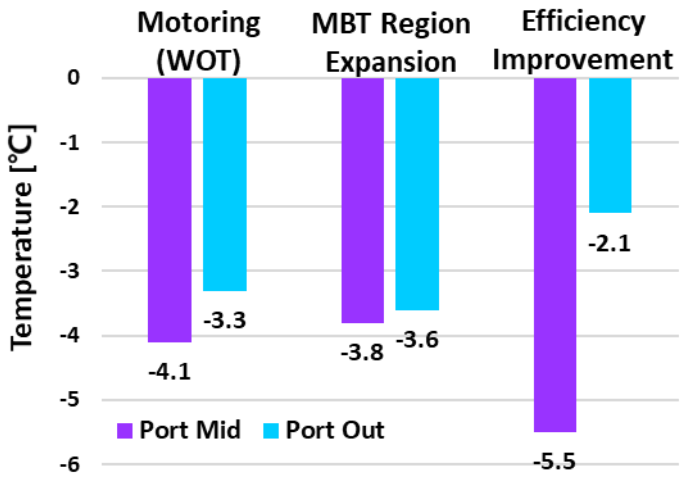

Figure 3.4.1 Port mid and port out temperature

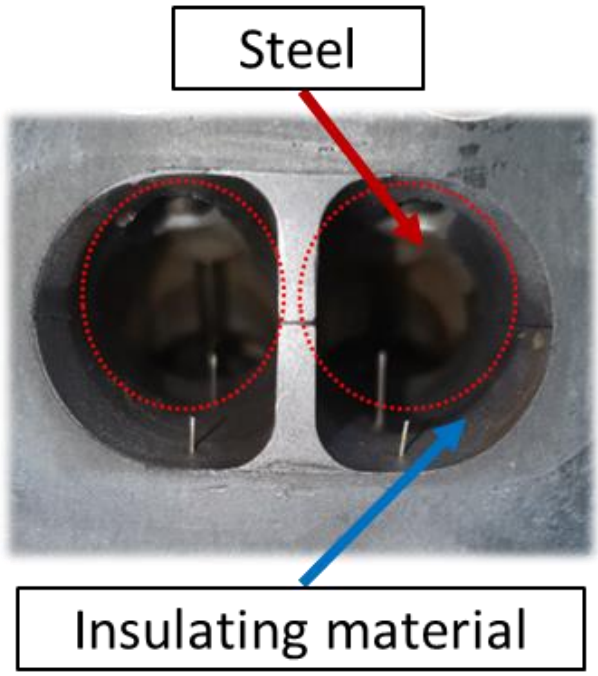

Figure 3.4.2 Internal structure of insulated intake port

3.5 CFD Simulation

To investigate the expected outcome when insulation was done perfectly, CFD simulation was done. First, to verify the reliability of CFD, result was compared between WOT motoring engine test and CFD simulation. CFD representing imperfect insulation in the real engine was done by only insulating the half of the intake port on the bottom. Even though there was a small discrepancy between absolute temperature of real engine data and CFD result (Figure 3.5.1), overall prediction of temperature reduction magnitude by insulation well matched in Figure 3.5.2. Especially at port out, which is the main interest in temperature reduction effect of insulation, result showed decent matching. Thereby assuming CFD result is trustworthy, simulation was conducted for full insulation on top and bottom.

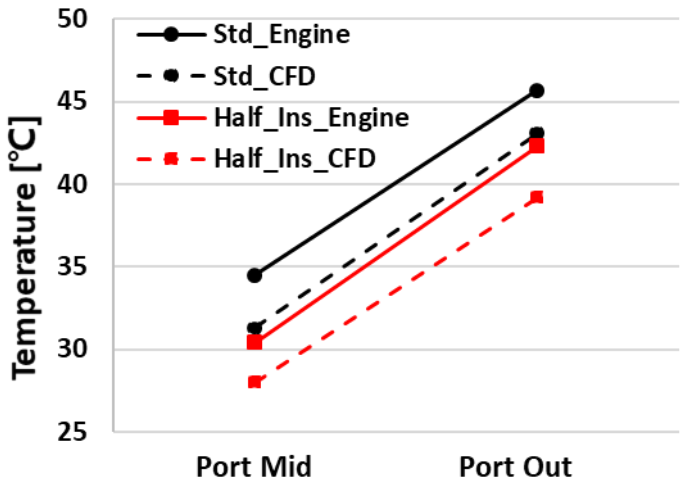

Figure 3.5.1 Experimental vs CFD port air temperature

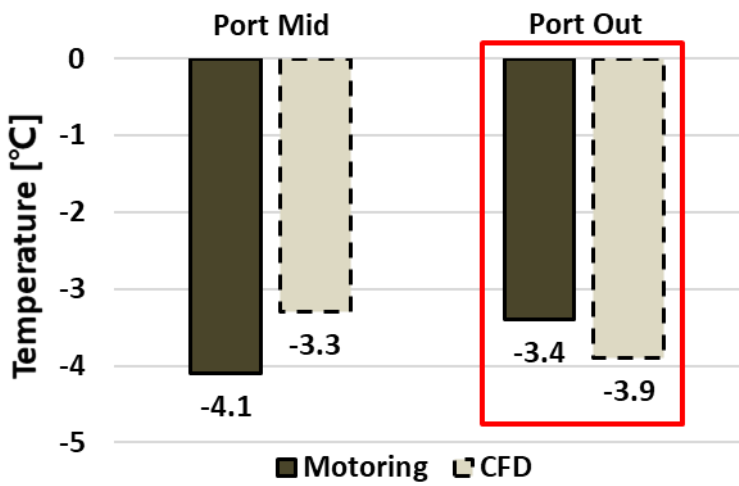

Figure 3.5.2 Experimental vs CFD port air temperature reduction

The difference in temperature gradient for standard, half-insulated, and full-insulated intake port was apparent during intake stroke, as shown in Figure 3.5.3. Difference in temperature reduction by half insulation and full insulation compared to standard port is illustrated in Figure 3.5.4. It was possible to observe that even with full insulation, temperature has slightly increased from intake port mid to port out because heat transfer occurred from intake valve, which was not insulated. At port out, compared to 3.9 ℃ reduction by half insulation, full insulation resulted in 14 ℃ fall that is 3.6 times more effective reduction. At knock prone operating condition, improved efficiency would be achievable by more efficient combustion with reduced knocking due to additional overall temperature reduction. In-cylinder temperature at TDC was reduced by 3.9 %, while pressure increased by 0.73 % at WOT condition (Figure 3.5.5). This implies that due to reduced temperature, volumetric efficiency increased, so more air mass was trapped. More fuel could be injected through enhanced volumetric efficiency, so maximum load expansion is also expected.

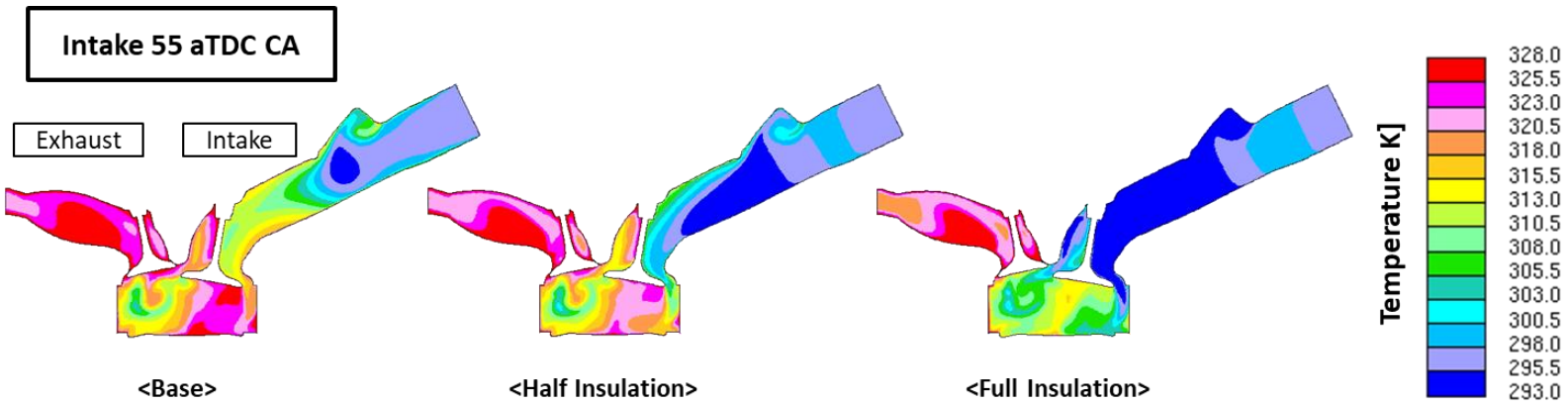

Figure 3.5.3 CFD simulation result of temperature gradient at standard, half-insulated, and full-insulated intake port

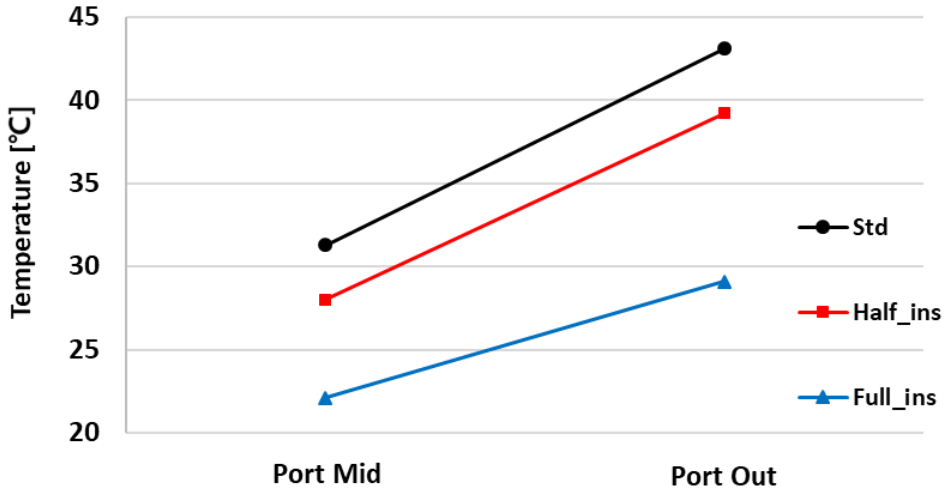

(a)

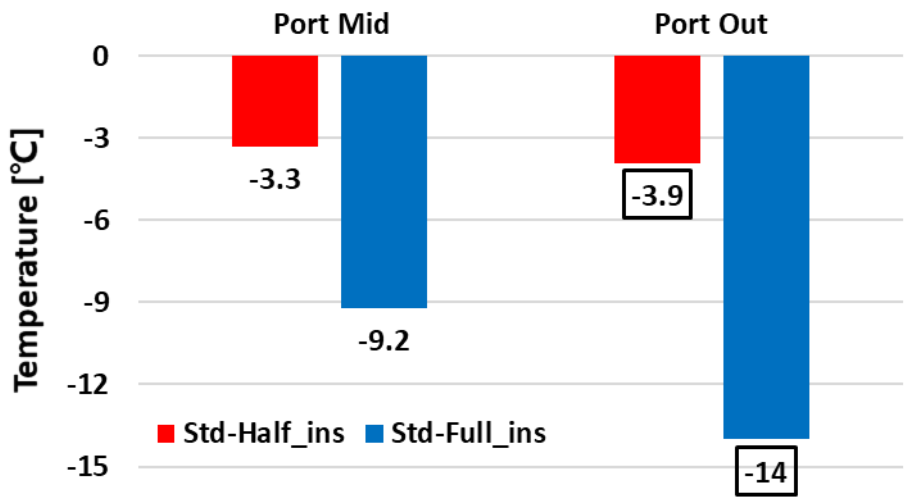

(b)

Figure 3.5.4 CFD simulation result of predicted temperature (a) and air temperature reduction compared to standard port (b)

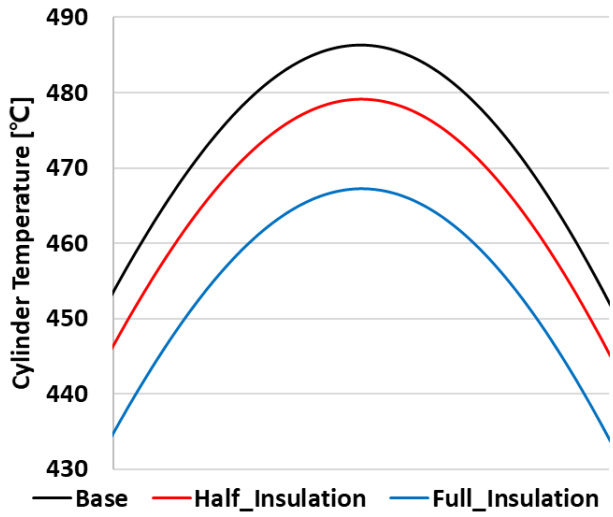

(a)

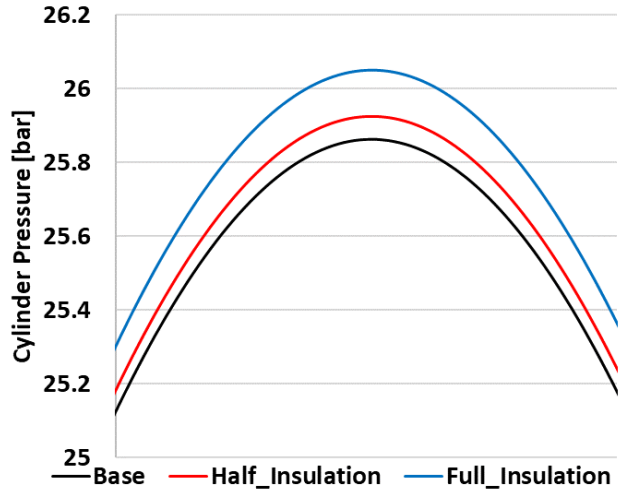

(b)

Figure 3.5.5 CFD simulation result of predicted in-cylinder temperature (a) and pressure (b) at TDC

Chapter 4. Results of Piston Cooling Oil-jet

4.1 Oil-jet Performance

4.1.1 Flow Rate of Undercrown Oil-jet

To analyze the effect of oil pressure and flow rate on combustion afterwards, it was first required to measure the performance of the oil-jets. Therefore, flow rate was measured at various oil pressures.

Two undercrown oil-jets with different outlet diameters of 1.7 mm and 1.1 mm were investigated (Figure 4.1.1). In overall, the measurement result shows that oil-jet with larger diameter had higher flow rate (Figure 4.1.2). However, diameter 1.7 mm oil-jet hardly had any flow below oil pressure of 1.5 bar. This is due to insufficient oil velocity. At constant oil pressure, oil-jet with larger area can inject larger amount of oil, but velocity slows down. At oil pressure below 1.5 bar, it is assumed that oil velocity was extremely slow in diameter 1.7 mm oil-jet, so the momentum of the oil was not enough to push the oil upward at the exit.

In addition, based on the flow rate and exit area, whether piston oil speed can exceed piston maximum speed at 1500 rpm and 2500 rpm was determined. Figure 4.1.3 demonstrates that diameter

1.7 mm oil-jet cannot follow 1500 rpm piston maximum speed at 2 bar and 2500 rpm piston maximum speed at 3 bar. In contrast, diameter 1.1 mm oil-jet did not have issue with catching up piston maximum speed, except for 2500 rpm at 1 bar. If injected oil velocity cannot overcome piston maximum speed, cooling effect is limited to only some portion of the cycle. Therefore, diameter 1.1 mm oil-jet that shows satisfactory performance in wide range of operating conditions was chosen for the experiments.

Figure 4.1.1 Diameter 1.7 mm (left) and 1.1 mm (right) undercrown oil-jet

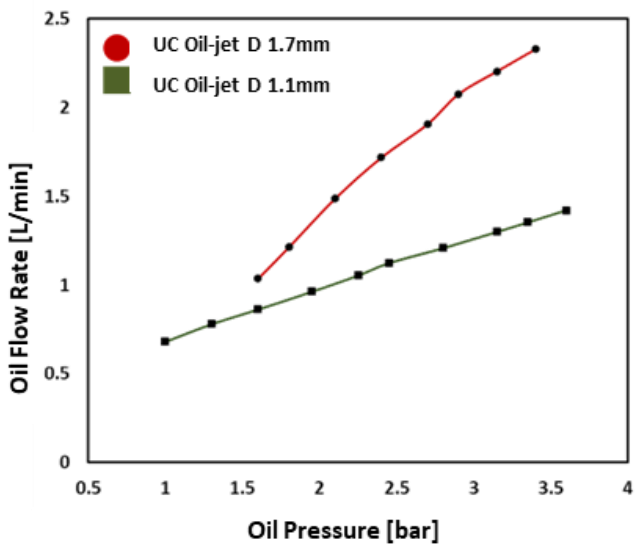

Figure 4.1.2 Undercrown oil-jet oil flow rate

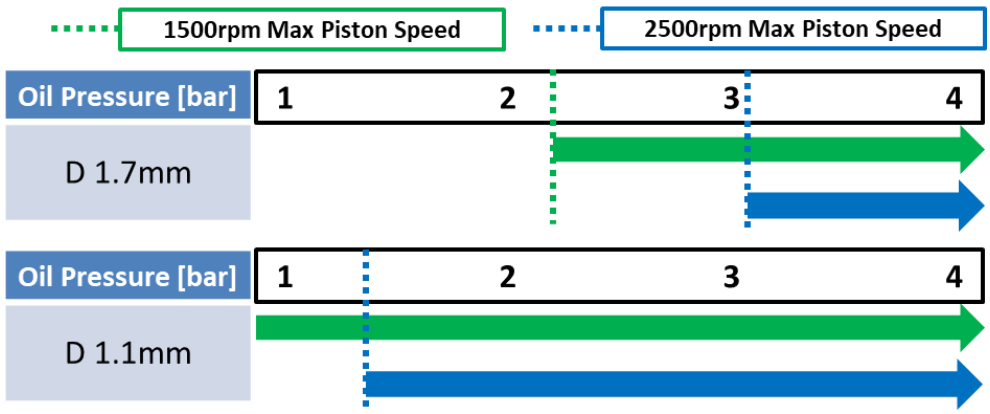

Figure 4.1.3 Undercrown oil-jet oil velocity sufficiency

4.1.2 Flow Rate of Cooling Gallery Oil-jet

Likewise, two cooling gallery oil-jets with different outlet diameters of 1.0 mm and 1.5 mm were tested for oil flow rate measurement (Figure 4.1.4). Both oil-jets had no problem with shooting oil, even at 1 bar (Figure 4.1.5). Similar to undercrown oil-jet, oil-jet with larger diameter exhibited larger oil flow rate at identical oil pressure. Even though oil velocity is not sufficient to reach 2500 rpm maximum piston speed for diameter 1.0 mm oil-jet, both oil-jets showed decent performance in overall (Figure 4.1.6).

Figure 4.1.4 Diameter 1.0 mm cooling gallery oil-jet

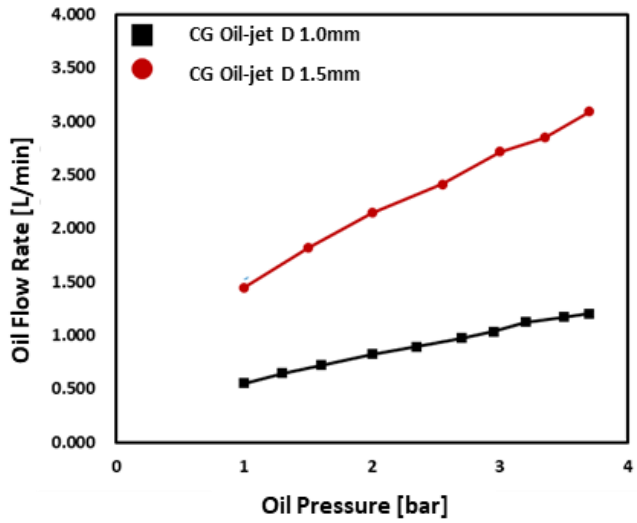

Figure 4.1.5 Cooling gallery oil-jet oil flow rate

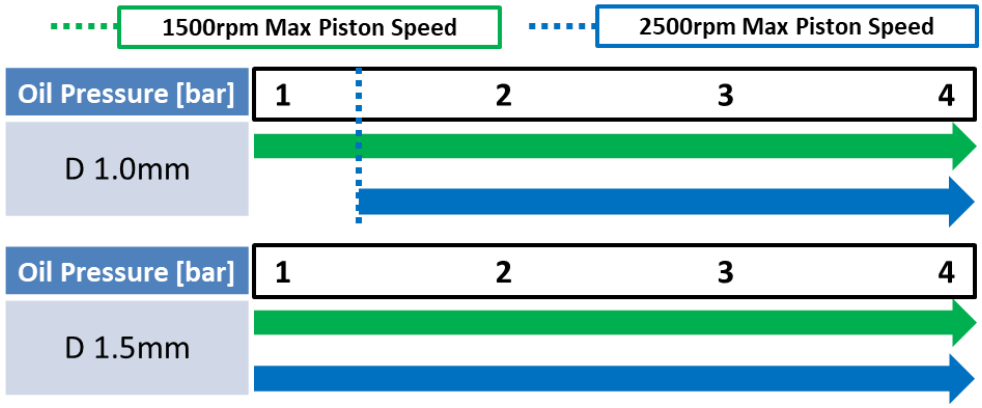

Figure 4.1.6 Cooling gallery oil-jet oil velocity sufficiency

4.1.3 Catching Efficiency of Cooling Gallery Oil-jet

In case of undercrown oil-jet, all injected oil are hit to undercrown of the piston, so entire amount is involved in cooling process. On the other hand, for cooling gallery oil-jet, oil serves its original purpose only if it passes through the cooling gallery. However, when experimentally investigated, it was observed that some portion of injected oil falls out, as shown in Figure 4.1.7. As a result, oil at the exit of cooling gallery has relatively weak stream (Figure 4.1.8). Looking at the figure, no targeting issue was found, so it implies that oil injected into the cooling gallery inlet is partially reflected back due to momentum and structural issue.

Because oil reflected back would not be involved in heat transfer inside of cooling gallery, it was needed to figure out the percentage of actual oil flow into cooling gallery out of entire oil injected from oil-jet, which is commonly referred to as catching efficiency. Catching efficiency was calculated by comparing the measured oil flow rate out of oil-jet in section 4.1.2 and additionally measured oil flow at exit of cooling gallery. The catching efficiency in Table 4.1.1 is the average at TDC and BDC. The result indicates that diameter 1.5 mm oil-jet performs superior to diameter 1.0 mm oil-jet. The reason for this result can be attributed to the fact that diameter 1.5 mm oil-jet is the upgraded version of diameter 1.0 mm

oil-jet; to improve the targeting accuracy, the oil-jet length was extended by 1 mm to align the oil-jet outlet to the cooling gallery inlet center. Because diameter 1.5 mm oil-jet exhibited better performance, especially at oil pressure 1 bar, it was chosen for combustion experiments.

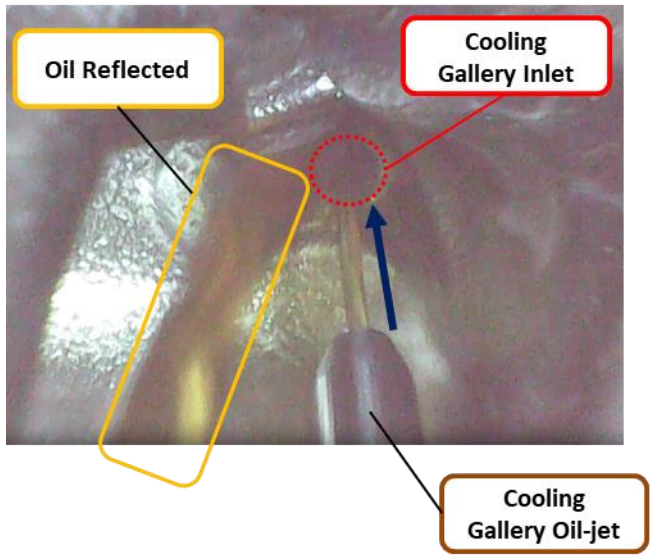

Figure 4.1.7 Cooling gallery inlet

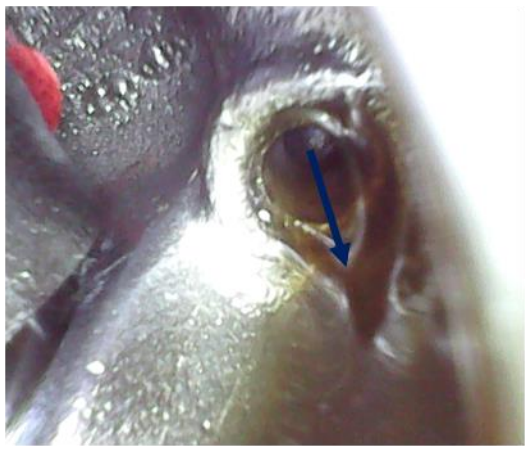

Figure 4.1.8 Cooling gallery outlet

Table 4.1.1 Catching efficiency for cooling gallery oil−jets

Oil Pressure [bar]	D 1.0mm Oil-jet	D 1.5mm Oil-jet
1	11.77	50.91
2	53.75	63.82
3.8	54.70	71.82

4.1.4 Equivalent Flow Rate Condition

To later examine the effect of flow rate, oil pressure conditions for each oil-jet types satisfying similar flow rate was chosen (Table 4.1.2). Undercrown oil-jet has approximately oil flow rate of 1.4 liter per minute at oil pressure of 3.8 bar. In case of cooling gallery, to determine the actual flow amount involved in heat transfer process in cooling gallery, flow rate out of oil-jet was multiplied by catching efficiency. At 2 bar, near 1.4 liter per minute oil flow rate was satisfied. For simultaneous injection, it was calculated by adding flow rate of undercrown oil-jet and that of cooling gallery with consideration of catching efficiency. Oil pressure 1 bar condition corresponded to 1.4 liter per minute in simultaneous injection. Since these three conditions are all near 1.4 liter per minute, they are referred to as equivalent flow rate case in analysis afterwards.

Table 4.1.2 Equivalent flow rate condition by oil-jet types

Oil-jet Type	Oil Pressure
Undercrown	3.8 bar
Cooling Gallery	2 bar
Simultaneous Injection	1 bar

4.2 Cooling Effect of Oil-jet

4.2.1 Cooling Loss at Identical Ignition Timing

When oil is injected by oil-jet to under the piston, heat transfer additionally occurs from in-cylinder and piston to oil. Therefore, oil temperature would rise, whereas in-cylinder temperature would drop. Compared to base condition (no oil-jet injection), oil temperature rose by 1.84 ℃ at 1500 rpm and 2.66 ℃ at 2500 rpm on average for all oil-jet types and oil pressures. Temperature rise was greater at 2500 rpm because for equal duration, more heat is released from larger number of cycles.

In case of in-cylinder, temperature reduction was measured by decline in pressure since they are correlated to each other (Figure 4.2.1). Pressure drop can be recalculated into IMEP loss and at same ignition timing, IMEP loss by oil-jet application represents cooling effect. In Figure 4.2.2, average IMEP losses for all oil pressures by each oil-jet type at two engine speeds are graphed. In the diagram, it can be clarified from the existence of IMEP losses that all oil-jets have cooling effect. Furthermore, it is noticeable from the magnitude of the losses that oil-jets are relatively more effective at cooling in-cylinder in order of simultaneous injection, cooling gallery, and undercrown oil-jets. Simultaneous injection was the most effective in

cooling due to large cooling oil coverage area. Cooling gallery oil-jet recorded higher cooling loss than undercrown due to structural differences that leads to more effective cooling, mentioned in Section 1.2.

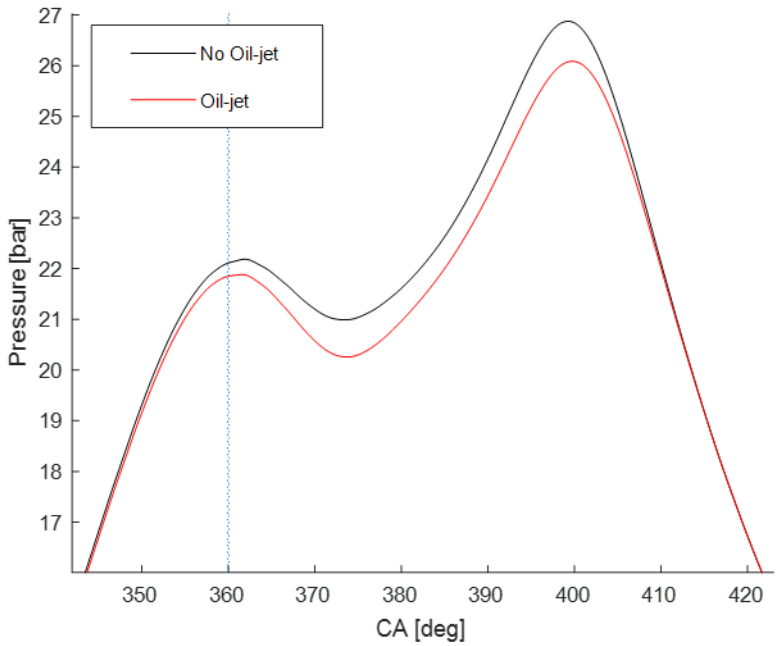

Figure 4.2.1 Pressure curve at identical ignition timing

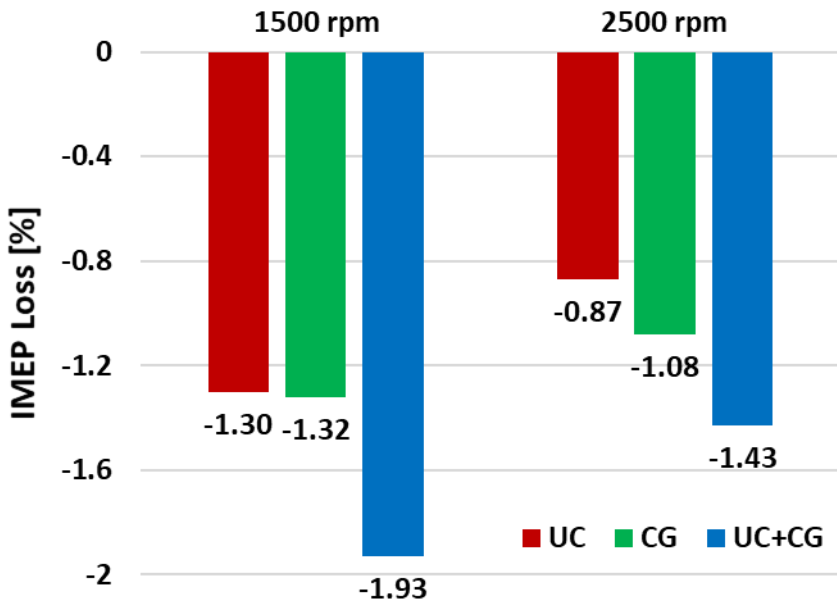

Figure 4.2.2 IMEP loss by oil-jet cooling at identical ignition timing

4.2.2 Loss Recovery by Ignition Timing Advance

Due to cooling effect of oil-jet, knocking was reduced from 10 % to about 2 %. Thus, ignition timing could be advanced as much as 2.2 CA, leading to more efficient combustion (Figure 4.2.3). For instance, peak pressure was increased and burn duration was shortened. As a result, efficiency improvement was possible. The detailed explanation will be followed in upcoming sections.

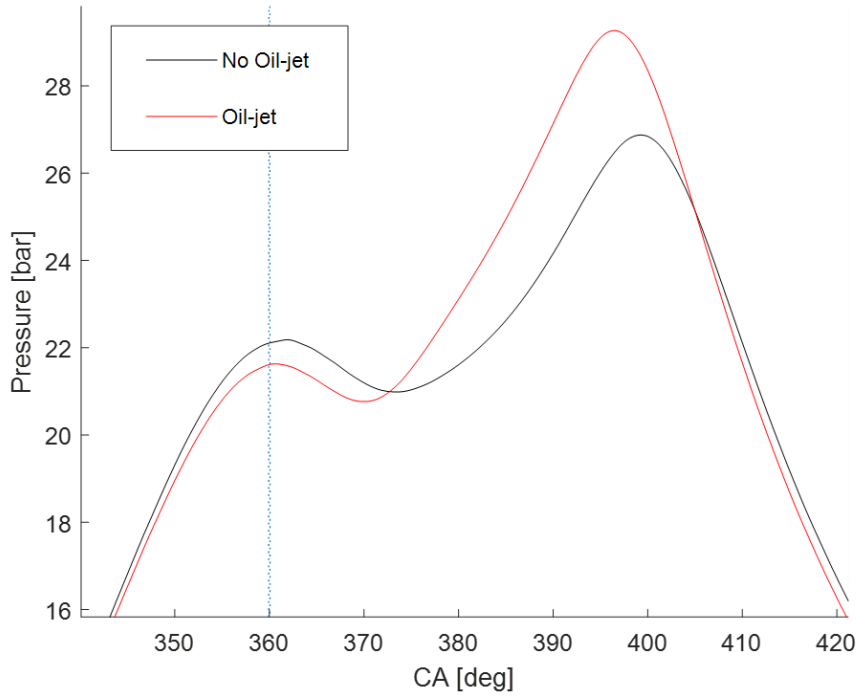

Figure 4.2.3 Pressure curve at advanced ignition timing by oil-jet

4.3 Efficiency Improvement at 1500 rpm

With undercrown oil-jet, ignition timing could be advanced by 0.7 or 0.8 CA due to reduced knocking from piston cooling (Figure 4.3.1). As a result, combustion took place in more efficient manner. For example, burn duration shortened by more than 0.3 CA and peak pressure increased by more than 0.55 bar. IMEP gain by more efficient combustion was highest for oil pressure 1 bar and decreased as oil pressure increased. It is inferred that with higher oil pressure, slightly more cooling loss has occurred with higher flow rate to extent that is not enough to further advance the ignition timing.

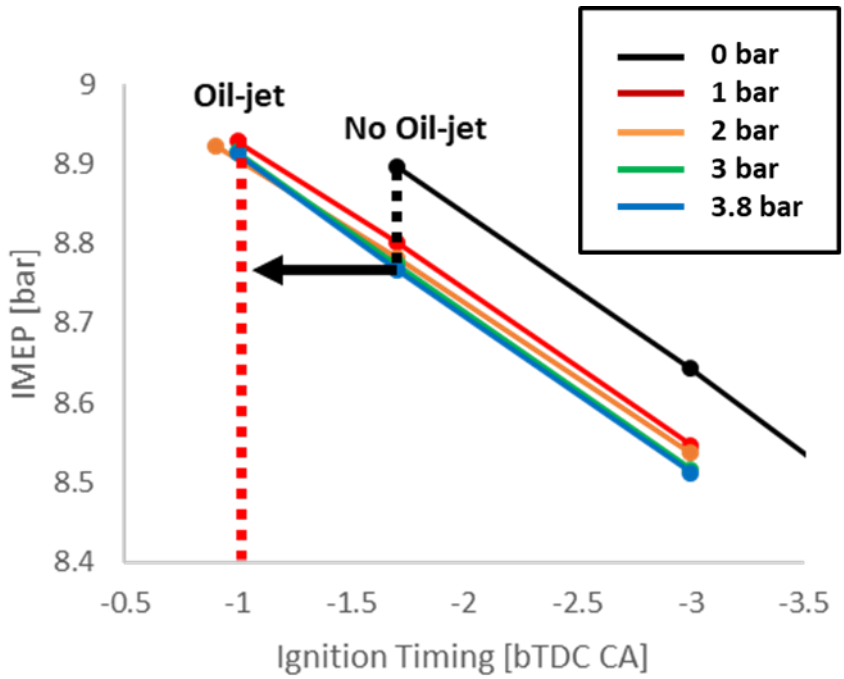

Figure 4.3.1 Effect of undercrown oil-jet on IMEP at 1500 rpm

Larger ignition timing advance was possible with cooling gallery oil-jet compared to undercrown oil-jet due to more effective cooling originating from structural difference mentioned previously (Figure 4.3.2). Also, unlike undercrown oil-jet, ignition advance increased with higher oil pressure. It is assumed that this phenomenon is due to insufficient cooling as only portion of injected oil is involved in cooling, which was checked by catching efficiency in Section 4.1.3. Accordingly, since more ignition advance is possible, burn duration shortening, peak pressure, and ultimately IMEP gain was larger in higher oil pressure.

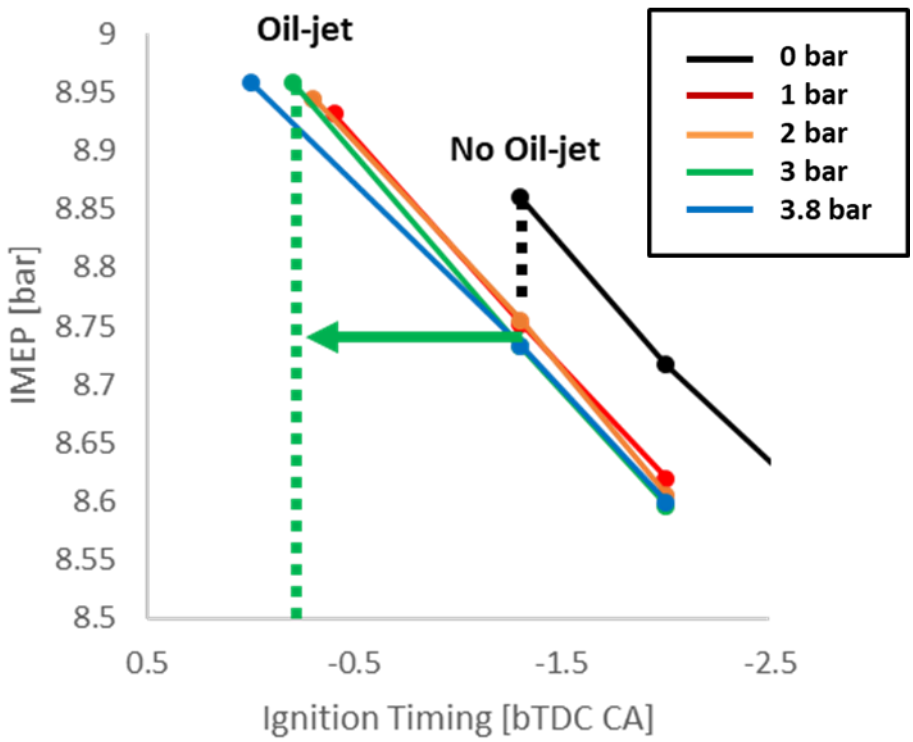

Figure 4.3.2 Effect of cooling gallery oil-jet on IMEP at 1500 rpm

When both oil-jets are applied simultaneously, 1.7 CA ignition timing advance was possible at 1 bar and 1.8 CA at other oil pressures by most effective cooling of the three oil-jet types. At highest oil pressure of 3.8 bar, peak pressure was recorded the highest and MFB50 located at most advanced angle. Due to this, the greatest IMEP gain was achieved.

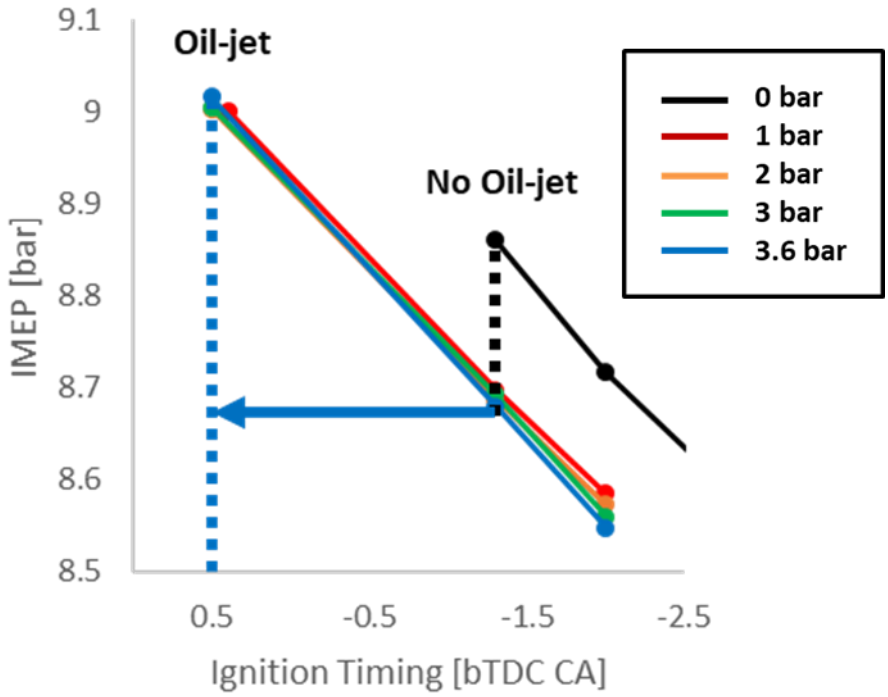

Figure 4.3.3 Effect of simultaneous injection on IMEP at 1500 rpm

IMEP gain by ignition timing advance from oil-jet cooling for all oil-jet types and oil pressures is depicted in Figure 4.3.4. Data points for equal oil flow rate of 1.4 liter per minute is marked as diamond. Difference in IMEP gain among different oil pressures for same oil-jet type is relatively smaller than difference between the oil-jet types. Also, at same oil flow rate, IMEP gain seems to be largely influenced by oil-jet type. Therefore, it is evident that IMEP gain is dominantly dependent on oil-jet type, rather than oil pressure or flow rate.

Both ignition timing advance amount and IMEP gain quantity was large in order of simultaneous, cooling gallery, and undercrown oil-jet (Figure 4.3.5). This coincides with the order of cooling effectiveness, found in Section 4.2.1. Therefore, it can be concluded that with more cooling, higher output from further advanced spark timing can be expected at this operating point.

Examining deeper into the sources of IMEP gain, majority of improvement was from compression and expansion strokes. In compression stroke, all three oil-jet types benefited from reduced work due to reduced working fluid temperature, as illustrated in Figure 4.3.6. Simultaneous injection benefited more due to higher cooling effectiveness. Regarding expansion stroke, the difference between oil-jet types was enlarged. With undercrown oil-jet, loss

was recorded. Compared to cooling loss, loss recovery from spark advance was not sufficient due to lowest ignition timing advance of the three types. In contrast, cooling gallery and simultaneous oil-jet had enough output recovery due to larger ignition timing advance from better cooling.

With equivalent fuel rate, IMEP was increased, so oil-jet had efficiency improvement effect. Also, the fact that efficiency improvement magnitude was larger for better cooling oil-jet suggests that cooling should be intensified in this operating condition.

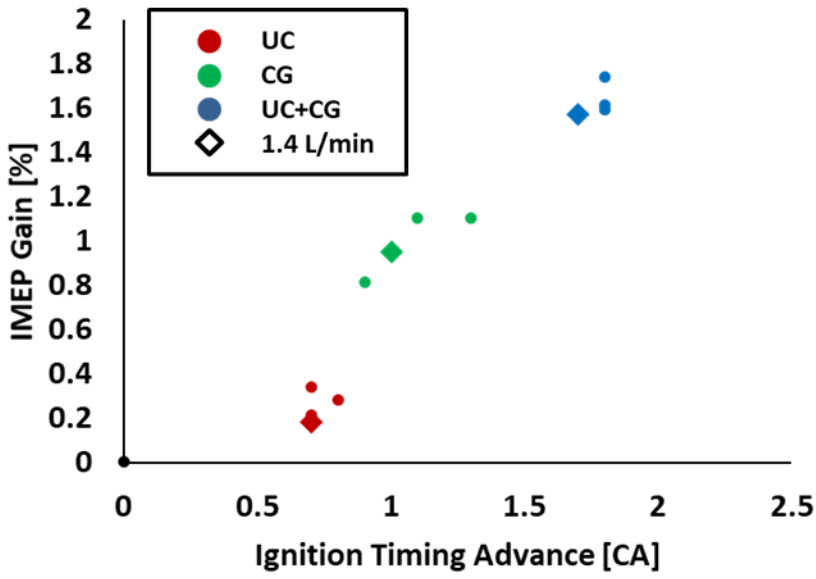

Figure 4.3.4 Effect of oil-jets on ignition timing and IMEP at 1500 rpm

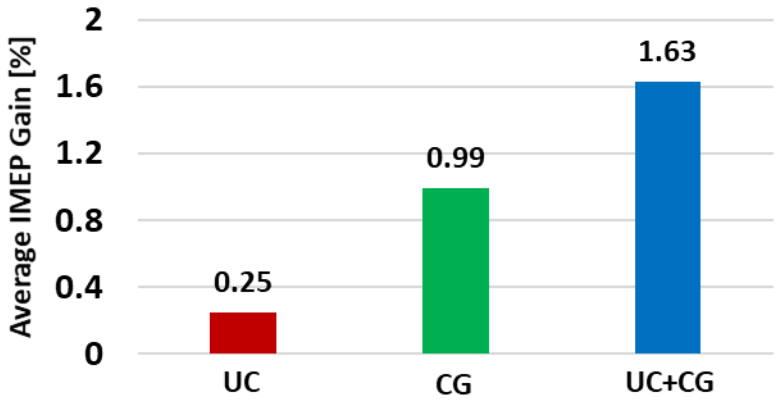

Figure 4.3.5 Average IMEP gain by oil-jet types at 1500 rpm

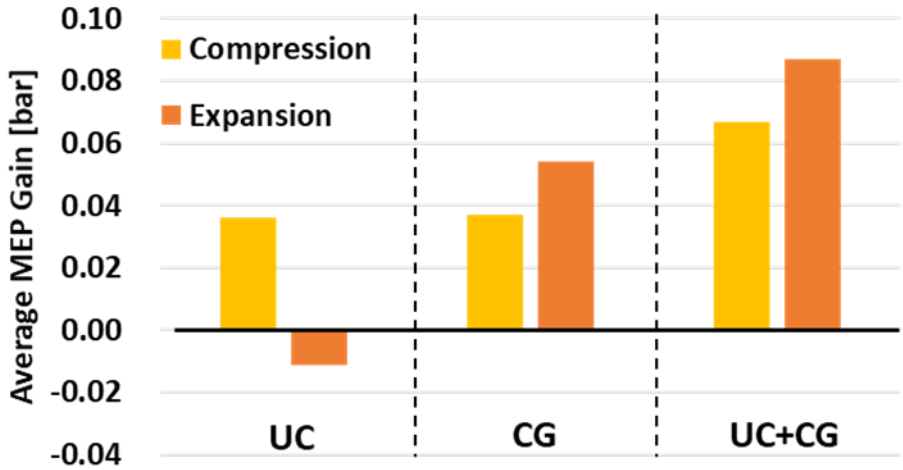

Figure 4.3.6 Average MEP gain by strokes at 1500 rpm

4.4 Efficiency Improvement at 2500 rpm

In 2500 rpm, spark timing advance by oil-jet cooling led to more efficient combustion and, thus, IMEP gain as well. Undercrown oil-jet with 1 bar oil pressure clearly showed smaller magnitude in ignition timing advance compared to higher pressure (Figure 4.4.1). This phenomenon, which is in contrary to 1500 rpm undercrown oil-jet case, is related to engine speed. At higher engine speed, faster oil speed is required to follow piston maximum speed. However, at 1 bar, the oil velocity was not sufficient relative to piston maximum speed as measured in Section 4.1.1. In other words, cooling was in action for only part of a cycle. Due to partial cooling, limited ignition timing advance was possible. Excluding 1 bar, similar pattern was observed as 1500 rpm in that higher pressure led to less IMEP gain as cooling loss aggravated with higher oil flow rate.

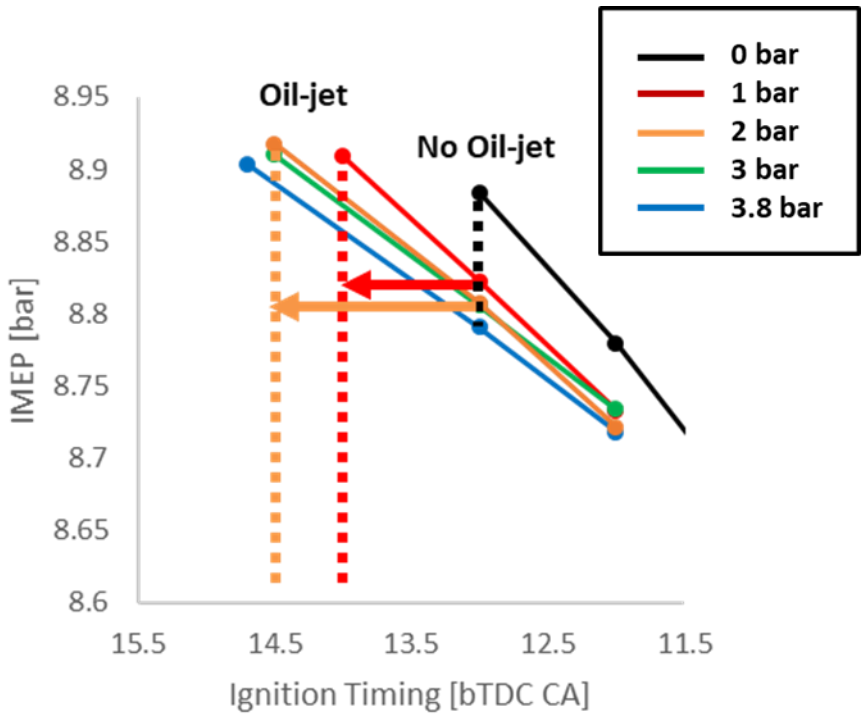

Figure 4.4.1 Effect of undercrown oil-jet on IMEP at 2500 rpm

Similar to cooling gallery oil-jet result in 1500 rpm, ignition timing advance quantity has gone up with increasing oil pressure (Figure 4.4.2). The same reason can be attributed for this phenomenon as Section 4.3.2. As a result, more efficient combustion, such as shortened burn duration, more advanced MFB50, and higher peak pressure, took place with rise in oil pressure. Eventually, higher IMEP gain was followed.

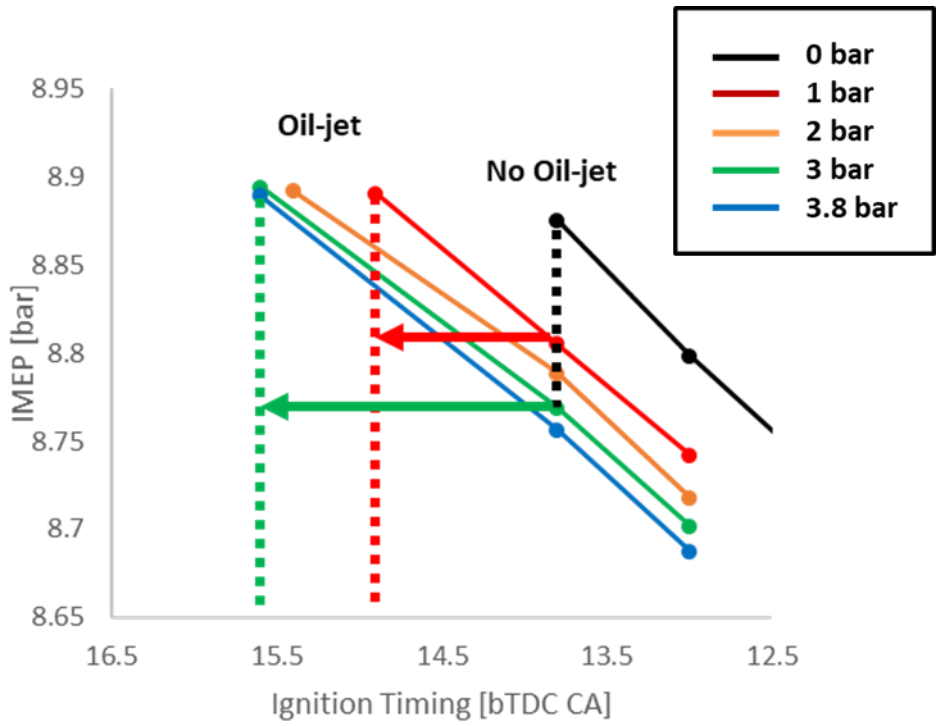

Figure 4.4.2 Effect of cooling gallery oil-jet on IMEP at 2500 rpm

Both undercrown oil-jet and cooling gallery oil-jet showed further ignition timing advance with higher oil pressure in 2500 rpm due to insufficient cooling time for each cycle at higher speed. Accordingly, simultaneous injection presented identical trend (Figure 4.4.3). At earlier ignition timing, burn duration took shorter time and, thus, MFB50 was advanced. Consequentially, higher IMEP gain was seen for higher oil pressure.

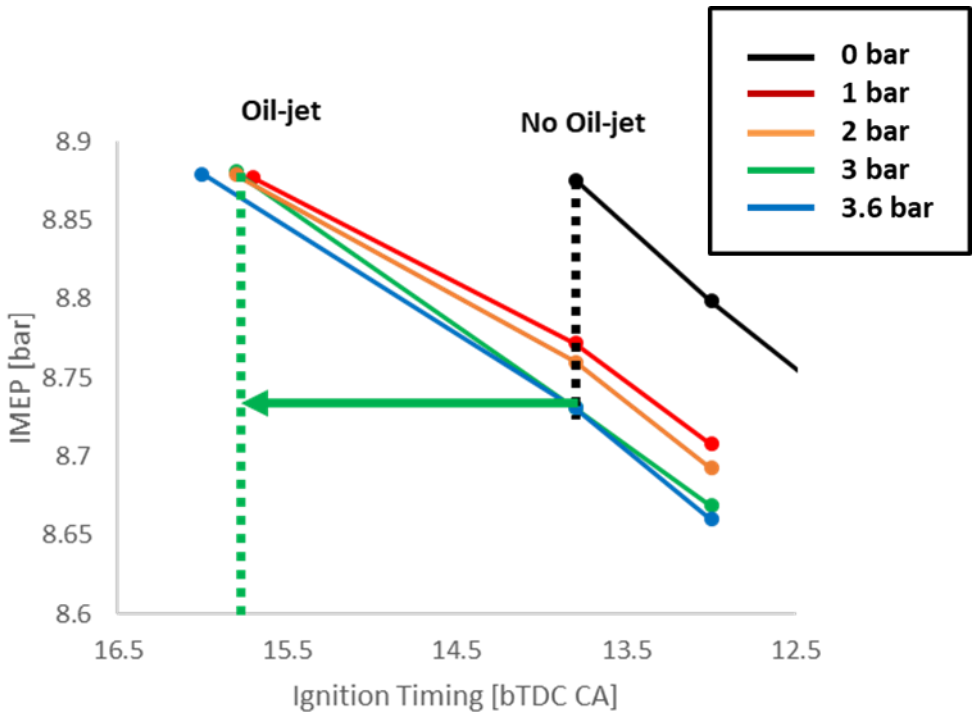

Figure 4.4.3 Effect of simultaneous injection on IMEP at 2500 rpm

In 2500 rpm, IMEP gain was not as great as 1500 rpm, shown in Figure 4.4.4. Oil-jet type still had dominant effect on IMEP gain over oil pressure and flow rate. However, the output increment was in reverse order of the oil-jet cooling effectiveness, which is an opposite trend from 1500 rpm (Figure 4.4.5). Undercrown oil-jet (0.29 %) was most effective in IMEP gain, followed by cooling gallery oil-jet (0.17 %) and simultaneous injection (0.03 %).

Figure 4.4.6 demonstrates that MEP gain was achieved during compression stroke as in 1500 rpm, but by reduced amount. The reduction originates from ignition timing. At 1500 rpm, spark occurs near TDC from 1.7 ATDC CA to 0.5 BTDC CA. Accordingly, combustion initiates after TDC. Therefore, throughout the entire compression stroke, pressure is kept lower than no oil injection case, leading to fully reduced compression work. However, at 2500 rpm, ignition is set between 13 to 16 BTDC CA, so combustion starts before TDC. Due to advanced spark timing when oil-jet is applied, pressure curve exceeds the base case and this leads to relatively increased compression work for part of the stroke. Thereby, only partial advantage was measured. Yet, overall trend in compression stroke was similar.

The opposite trend compared to 1500 rpm was mainly the result of expansion stroke. MEP gain at expansion reduced and

converted to loss for oil-jet with better cooling impact. This finding implies that extensive cooling is demerit to raising output. Still, despite small amount, IMEP increased with fixed fuel rate, so efficiency was improved.

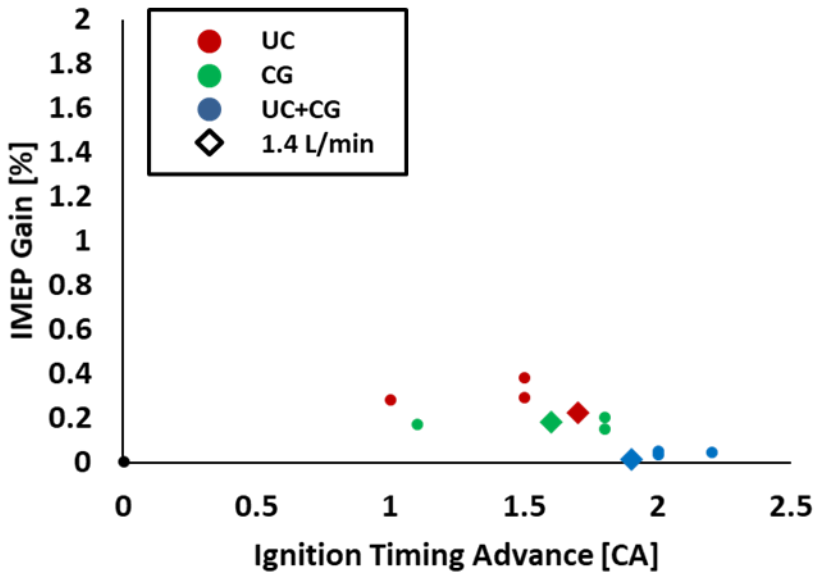

Figure 4.4.4 Effect of oil-jets on ignition timing and IMEP at 2500 rpm

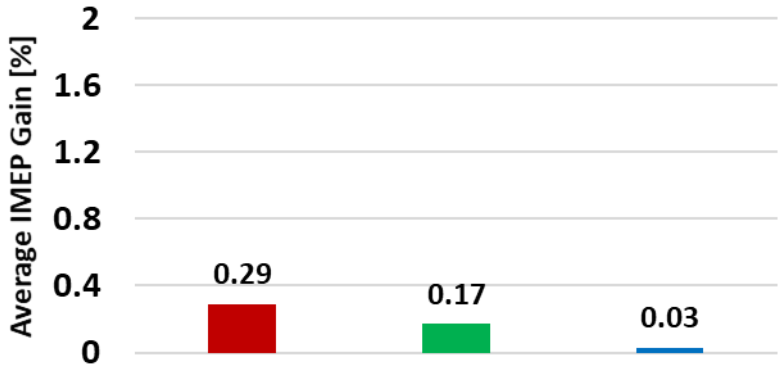

Figure 4.4.5 Average IMEP gain by oil-jet types at 2500 rpm

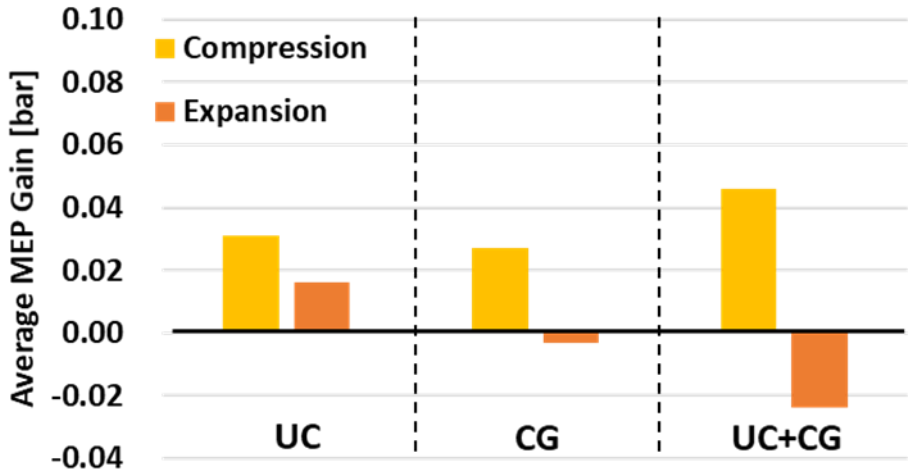

Figure 4.4.6 Average MEP gain by strokes at 2500 rpm

4.5 Analysis

Compared to 2500 rpm, extensive efficiency enhancement was enabled at 1500 rpm. This phenomenon can be attributed to ignition timing and MFB50 location, represented in Table 4.5.1. At 1500 rpm, internal flow and flame propagation speed is relatively slow due to lower engine speed. Therefore, knock is easily generated, enforcing retarded ignition timing to near TDC. Accordingly, MFB50 is retarded to between 30 to 33.1 ATDC CA, which is far away from MBT. In this case, if spark timing is advanced, output rises significantly as explained by blue line in Figure 4.5.1. With more cooling, larger IMEP gain from even further ignition timing advance is possible. Therefore, oil-jet with better cooling effect led to higher efficiency improvement, indicated by increasing trend from left to right in Figure 4.5.2.

In contrast, at 2500 rpm, knock is relatively suppressed due to faster internal flow and flame propagation speed in higher speed. MFB50 for 2500 rpm experiment was located between 14.3 to 17.3 ATDC CA, which is comparatively closer to MBT. At this range, it is hard to expect equivalent output increment as 1500 rpm, illustrated by red line in Figure 4.5.1. Therefore, while output recovery by ignition timing advance is limited, cooling loss deteriorates for oil-jet with better cooling effectiveness. As a result, oil-jet with more effective cooling was found to be more detrimental in improving

efficiency, depicted by decreasing trend in Figure 4.5.2.

The fact that the different magnitude and opposing trend appeared at two engine speed conditions implies the need for appropriate oil-jet strategy at different engine operating points.

Table 4.5.1 Ignition timing and MFB50 at two engine speeds

Engine Speed [rpm]	Ignition Timing [bTDC CA]	MFB 50 Range [aTDC CA]
1500	-1.7 ~ 0.5	30.0 ~ 33.1
2500	13.0 ~ 16.0	14.3 ~ 17.3

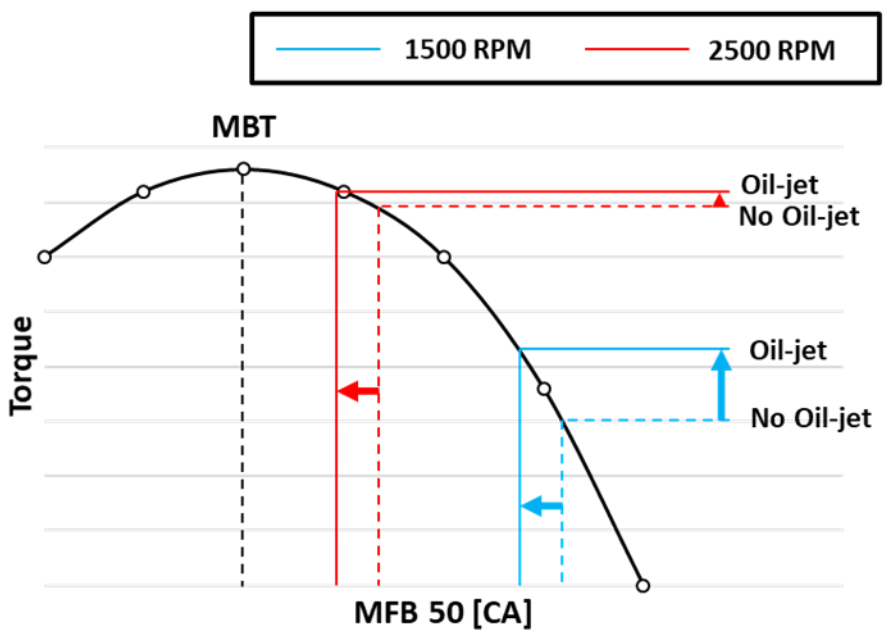

Figure 4.5.1 Output gain by ignition timing advance at different MFB50

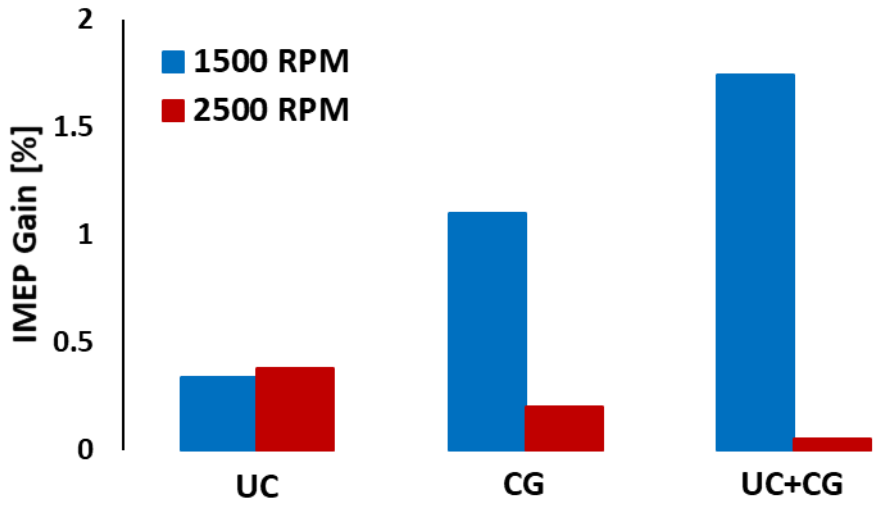

Figure 4.5.2 Average IMEP gain by oil-jets types at two engine speeds

Chapter 5. Conclusions

Improvement of engine efficiency is critical to satisfy the regulations, but has been hindered by knocking phenomenon. To reduce knock, temperature drop of working fluid is essential. Therefore, thermal boundary conditions were changed at intake port and piston. Intake port was modified by replacing part of the body with insulating material, so heat transfer was partially blocked from intake port to incoming air. Temperature of the air-fuel mixture inside of combustion chamber was reduced by intensifying cooling with oil injection to piston from oil-jets.

The temperature reduction effect of intake port insulation was first checked at WOT motoring case. Total of 3.4 ℃ reduction at port out was measured. With this effect confirmed, combustion experiments were followed.

First, expansion of MBT region was investigated by finding the borderline point where MBT (MFB50 at 8 ATDC CA) coincides with KLSA. Above this point, knocking is excessive that ignition timing cannot be advanced to MBT. Compared to standard port, 3.6 ℃ reduction at port out was possible with the insulated port. Due to accordingly less knocking tendency, fuel rate was increased and ignition timing was adjusted to satisfy the requirements. MBT region

boundary point was ultimately found and this point was 1.79 % higher in IMEP compared to standard port case. Between the MBT region borderline points of standard port and insulated port, only insulated port would maintain maximum efficiency, so it was indirectly investigated that efficiency improvement is possible with the intake port insulation in certain load range.

Next, to directly compare the efficiency, fixed fuel rate experiment was conducted. By temperature reduction at port out, ignition timing could be further advanced by 1.6 CA. As a result, more efficient combustion took place and, thus, modest MEP gain was possible at expansion stroke. Total of 0.29 % IMEP increase was accomplished. At identical given fuel amount, output was larger, so efficiency improvement was achieved with the insulated intake port.

The insulation was not done perfectly due to manufacturing issue caused by complex internal design of intake port. Thus, only partial effect of insulation was expected. Throughout motoring and combustion experiments, it was observed that the effect of temperature reduction weakens as air moves from port mid to port out, meaning heat transfer is occurring along the path. To see possible maximum effect if insulation was done completely, CFD simulation was run. CFD simulation of fully insulated intake port was conducted and resulted in 3.6 times better air temperature reduction

effect than half-insulated case. Accordingly, enhanced efficiency by knocking suppression and load expansion by higher volumetric efficiency is expected.

Efficiency improvement was possible with piston cooling oil-jet as well. Likewise, cooling effect of oil-jet was first verified. Experiments were conducted with fixed fuel rates at two engine speeds. At same ignition timing, IMEP drop equals to cooling loss, so it was concluded that oil-jets were effective in cooling in order of simultaneous injection, followed by cooling gallery and undercrown oil-jets.

From reducing knocking by cooling effect of oil-jet, ignition timing could be advanced to new KLSA and more efficient combustion was achieved. Consequentially, IMEP gain was possible, but by different magnitude and trend at two different engine speeds.

At 1500 rpm combustion experiment, it was found that oil-jet type has dominant influence over oil flow rate or injection pressure. Also, better cooling oil-jet led to further advanced ignition timing and higher IMEP gain. All oil-jet types could benefit during compression stroke due to less work done to engine by reduced temperature from cooling. The difference in quantity of IMEP gain between oil-jet types mainly originated from expansion stroke. Undercrown oil-jet,

which is least effective in cooling, recorded loss because advantage from ignition timing advance was not sufficient enough to recover cooling loss. In contrast, other two types gained MEP by larger ignition timing advance.

At 2500 rpm, dominance of oil-jet type over oil flow rate and pressure was equally observed. Furthermore, ignition timing advance was greater in order of cooling effective oil-jet types. However, IMEP gain was in reverse order, mainly due to opposite trend in expansion stroke. Benefit during compression stroke was smaller compared to 1500 rpm.

The difference in magnitude and trend of IMEP gain by oil-jet types is closely related to ignition timing. At 1500 rpm, engine is prone to high knocking tendency since internal flow motion and flame propagation speed is slow. As a result, ignition timing is retarded to near TDC, which makes MFB50 location far away from MBT timing. At point distant from MBT, relatively large output gain is possible with ignition timing advance. Therefore, better cooling oil-jet even could gain significantly higher IMEP gain. On the other hand, 2500 rpm relatively has strong suppression to knocking by higher internal flow motion and flame propagation speed, enabling ignition timing at closer point to MBT. Around this region, not only IMEP gain by oil-jet cooling is limited in quantity, but also additional ignition timing by

more effective oil-jet cannot lead to significant extra output increase. Therefore, at this test condition, better cooling oil-jet only exacerbated cooling loss, resulting in deteriorating overall IMEP gain trend.

Diverse magnitude and trend in IMEP gain by oil-jet types and engine operating conditions indicate the need for appropriate oil-jet strategy adjusted for each engine operating condition. Regardless, all test cases resulted in favorable outcome compared to base condition in respect to efficiency. Because experiment was conducted with fixed fuel rate, it can be concluded that implementation of piston cooling oil-jet has advantage on efficiency improvement.

In conclusion, this study experimentally investigated the effect of intake port insulation and piston cooling oil-jet on engine efficiency improvement and confirmed the meaningful relationship. It is expected that the results would contribute to automotive industry as a guidance to development of higher efficiency engine, which is urgently needed to satisfy the regulations and protect the environment.

Bibliography

[1] Ritchie, H. and Roser, M. CO2 and Greenhouse Gas Emissions. Our World in Data. 2019.

[2] Yang, Z. Overview of Global Fuel Economy Policies. ICCT, 2018.

[3] Worldwide Emission Standards Passenger Cars and Light Duty Vehicles 2018|2019. Delphi, 2018.

[4] Imaoka, Y., Shouji, K., Inoue, T., and Noda, T. A Study of Combustion Technology for a High Compression Ratio Engine: The Influence of Combustion Chamber Wall Temperature on Knocking. SAE Int. J. Engines 9(2):2016, doi:10.4271/2016-01-0703.

[5] Uchihara, K., Ishii, M., Nakajima, H., and Wakisaka, Y. A Study on Reducing Cooling loss in a Partially Insulated Piston for Diesel Engine. SAE Technical Paper 2018-01-1276, 2018, doi:10.4271/2018-01-1276.

[6] Maeyama, K., Yoshio, Y., Komatsu, H., Terao, A., Daicho, H., Sato, K., Harada, Y., Shibata, M. New 1.0 Liter Three-Cylinder Turbocharged Gasoline Direct Injection Engine from Honda. Aachen Colloquium Automobile and Engine Technology, 2017.

[7] Kuboyama, T., Moriyoshi, Y., Iwasaki, M., Hara, J. Effect of Coolant Water and Intake Air Temperatures on Thermal Efficiency of a Spark Ignition Engine. SICE Annual Conference, 2013.

[8] Chhalotre, S., Baredar, P., and Soni, S. Experimental Investigation of the Effects of Insulated Air Intake System on the Performance of Naturally Aspirated MPSEFI Spark Ignition Engine. AIP Conference Proceedings 2039, 020001. 2018, doi: 10.1063/1.5078960.

[9] Anderson, D. The Effects of Ceramic Port Insulation on Cylinder Head Performance in a Diesel Engine. SAE Technical Paper 961745, 1996.

[10] Yoshida, N. Development of New I4 2.5L Gasoline Direct Injection Engine. SAE Technical Paper 2019-01-1199, 2019, doi:10.4271/2019-01-1199.

[11] Birtok-Baneassa, C., Ratiu, S., and Heput, T. Influence of Intake Air Temperature on Internal Combustion Engine Operation. IOP Conf. Ser.: Mater. Sci. Eng. 163 012039, 2017, doi:10.1088/1757-899X/163/1/012039.

[12] Hakansson, E. Intake Port Isolation for Direct Injected Turbo Charged Gasoline Engines. Chalmers University of Technology, 2011.

[13] Martins Leites, J., De Camargo, R. Articulated Piston Cooling Optimization. SAE Technical Paper 930276, 1993.

[14] Thiel, N., Weimar, H., and Kamp, H. Advanced Piston Cooling Efficiency: A Comparison of Different New Gallery Cooling Concepts. SAE Technical Paper 2007-01-1441, 2007.

[15] Luff, D., Law, T., Shayler, P. and Pegg, I. The Effect of Piston Cooling Jets on Diesel Engine Piston Temperatures, Emissions and Fuel Consumption. SAE Int. J. Engines 5(3):2012, doi:10.4271/2012-01-1212.

[16] Deng, L., Liu, Y., Wang, Z., Liu, S., and Zhang, J. Optimization of the Location of the Oil Cooling Gallery in the Diesel Engine Piston. The Open Mechanical Engineering Journal, 10, 126-134, 2016, doi: 10.2174/1874155X01610010126.

[17] Wang, P., Liang, R., Yu, Y., Zhang, J., Lv, J., and Bai, M. The flow and heat transfer characteristics of engine oil inside the piston cooling gallery. Applied Thermal Engineering 115, 620-629, 2017.

[18] Bush, J. and London, A. Design Data for "Cocktail Shaker" Cooled Pistons and Valves. SAE Technical Paper 650727, 1965.

국 문 초 록

전세계적으로 자동차에 대한 규제들이 엄격해지고 있으며, 이는 엔진의 효율 향상을 요구한다. 하지만, 노킹 현상은 엔진에 영구적이고 심각한 손상을 입힐 수 있으므로, 보다 효율적인 엔진 개발에 방해물로 작용하였다. 노킹은 엔진 내부에서 일을 하는 유체의 온도를 줄임으로써 저감 시킬 수 있고, 이는 엔진의 열 경계 조건을 변화를 주어 이뤄낼 수 있다.

본 연구에서는, 열 경계 조건 변경 방법으로 흡기 포트 단열과 피스톤 냉각 오일젯을 사용하였다. 흡기 포트 단열은 지극히 낮은 열 전도율을 가지는 소재를 통해 새로운 흡기로의 열 전달을 대부분 막을 수 있다. 피스톤 냉각 오일젯 적용 시, 연소실 내부에서 엔진 오일로 냉각을 강화시켜 실린더 내부 온도가 저감된다. 위의 두가지 방법들이 엔진 효율 향상 시킬 수 있는지 실험을 통해 확인해보았다.

단열 처리된 흡기 포트 사용을 통해 흡기 온도 하락 효과를 확인할 수 있었다. 따라서, MBT 영역을 확장시켰으며, 연료량 고정 실험에서 효율 향상된 결과를 얻었다. 복잡한 흡기 포트 내부 설계로 인해, 단열 처리를 완벽하게 할 수 없었다. 따라서 완벽한 단열 처리 시의 기대 효과를 예상하기 위해, CFD 시뮬레이션을 진행하였다. 해당 결과는 더욱 효과적인 공기 온도 저감과 체적 효율 증가를 나타내었다.

피스톤 냉각 오일젯은 연료량 고정한 채로 두가지의 엔진

속도에서 실험을 진행하였다. 오일젯 유형이 오일 압력과 유량보다 지배적인 효과를 가졌다. 또한, 다양한 오일젯이 공통적으로 효율 향상에 긍정적인 영향을 미쳤지만, 상승 규모나 경향성은 두가지 엔진 속도에서 상반되는 성향을 보였다. 이를 통해, 각 엔진 운전 조건에 적합한 오일젯 사용 전략이 필요하다는 점을 알 수 있었다.

결과적으로, 흡기 포트와 피스톤에서의 열 경계 조건 변화를 통한 엔진 효율 향상 효과를 본 연구에서 확인하였다. 이 결과들이 다양한 이유들로 인해 강력하게 요구되고 있는 고효율 엔진 개발에 도움이 될 것으로 예상된다.

주요어 : 효율 향상, 열 경계 조건, 흡기 포트 단열, 피스톤 냉각 오일젯, 쿨링갤러리, 언더크라운, SI 엔진

학번 : 2018-27312